Mathematical Modeling and Optimization of Run Parameters of Crystallization Analysis Fractionation (CRYSTAF)

Master Thesis

by

Michael FISCHLSCHWEIGER, BSc

prepared at the

Polymer Competence Center Leoben GmbH

submitted to the

Institut of Chemistry of Polymeric Materials
University of Leoben

Thesis Supervisor: Ao.Univ.-Prof.Dipl.-Chem.Dr.rer.nat. Nicolai Aust

Academic Advisor: Ao.Univ.-Prof.Dipl.-Chem.Dr.rer.nat. Nicolai Aust

Leoben, August 2009

Aufgabenblatt zur Masterarbeit
von Herrn Michael FISCHLSCHWEIGER, BSc

Eine Vielzahl technischer Kunststoffe besteht aus Blends von Polypropylen-Copolymeren mit entsprechenden Modifiern. Die Gebrauchseigenschaften eines jeden Kunststoffes werden sowohl durch die molekularen Parameter seiner Komponenten (z.B. Molmasse und deren Verteilung, Zusammensetzung des Copolymeren), als auch durch seine Phasenzusammensetzung und Morphologie bestimmt.

Die genaue Kenntnis über den Einfluß jedes dieser Parameter auf die Gebrauchseigenschaften ist daher unerläßlich für eine gezielte Entwicklung neuer Kunststoffe mit einem geforderten Anwendungsprofil. Hierfür ist eine leistungsstarke Analytik erforderlich, die Aufschluß über die Zusammensetzung bereits kommerziell erhältlicher, als auch neu zu entwickelnder Kunststoffe gibt.

Zur Phasenseparation und –analyse werden heute hauptsächlich zwei Verfahren angewandt: Temperature Rising Elution Fractionation und Crystallization Analysis Fractionation (CRYSTAF). Während ersteres Verfahren bzgl. Optimierung der Versuchsparameter bereits sehr gut untersucht ist, ist die Optimierung der Methode der CRYSTAF noch in zahlreichen Punkten lückenhaft.

Ziel der Arbeit ist es, die wichtigsten Einflußparameter eines CRYSTAF-Prozesses zu erfassen und mittels statistisch-mathematischer Methoden auszuwerten. Aus den hieraus gewonnenen Erkenntnissen ist ein optimiertes Verfahren zur Phasentrennung von Polypropylen-Blends mittels CRYSTAF zu entwickeln. Alle relevanten Faktoren und deren Einfluß sind genau zu dokumentieren, zu interpretieren und in Form einer wissenschaftlich einwandfreien Abhandlung zusammenzufassen.

Leoben, 01. April 2009

(Ao.Univ.Prof. Dr.rer.nat. Nicolai Aust)

Eidesstattliche Erklärung

Ich erkläre an Eides statt, dass ich diese Arbeit selbstständig verfasst, andere als die angegebenen Quellen und Hilfsmittel nicht benutzt und mich auch somit keiner unerlaubten Hilfsmittel bedient habe.

Michael Fischlschweiger, BSc

Leoben, am 21.08.2009

Acknowledgement

The author expresses his gratitude to Ao. Univ.-Prof. Dr.rer.nat. Nicolai Aust from the Institute of Chemistry of Polymeric Materials (University of Leoben,Austria), for supervising the Master Thesis, finding always time for inspiring discussions and chemical instructions.

Special thanks are due to Ao. Univ.-Prof. Dr.phil. Eduard R.Oberaigner from the Institute for Mechanics (University of Leoben,Austria) for helpful instructions in physical and mathematical questions.

Further the author thanks the Laboratory of Fluid Chromatography at the Institute of Chemistry of Polymeric Materials at the University of Leoben, especially Cornelia Kock and Thomas Ehgartner for supporting the experimental investigations.

For fruitful discussions and physical interpretations of the results of the underlying thesis the author thanks Ass.-Prof. Dr. Siripon Anantawaraskul from the Department of Chemical Engineering at the Kasetsart University (Bangkok,Thailand).

Parts of the research work of this Master Thesis were performed at the Polymer Competence Center Leoben GmbH (PCCL,Austria) within the framework of the Kplus program of the Austrian Ministry of Traffic, Innovation and Technology with contributions by the University of Leoben and Borealis GmbH (Linz,Austria). The PCCL is funded by The Austrian Government and the State Governments of Styria and Upper Austria.

Abstract

A sample independent statistic mathematical model was developed which describes the quality of separation of polymer blends by Crystallization Analysis Fractionation (CRYSTAF). By coupling the abstract model with experimental data, factors influencing the non-equilibrium CRYSTAF separation process of heterophasic polypropylene copolymers were determined. It could be shown that the stirring speed during CRYSTAF process strongly influences the quality of separation and thus the quality of the CRYSTAF profile obtained for a certain polymer. A new optimal fractionation method for CRYSTAF was designed which leads to CRYSTAF profiles of high quality. The results of the model were experimentally verified by application of the new method to three different polyolefin blends.

Kurzfassung

Zur qualitativen Beschreibung der Phasenseparation von Polyolefin-Blends durch eine kristallisierbarkeitskontrollierte Charakterisierungstechnik, Crystallization Analysis Fractionation (CRYSTAF), wurde ein probenunabhängiges statistisch mathematisches Modell entwickelt. Durch die Kopplung experimenteller Daten mit dem abstrahierten Modell wurden die Einflussfaktoren auf den Nichtgleichgewichts-Separationsprozess bei CRYSTAF-Analysen für heterophasische Polypropylen-Copolymere bestimmt. Dadurch konnte gezeigt werden, dass die Rührergeschwindigkeit während der CRYSTAF- Charakterisierung die Separationsqualität und somit das CRYSTAF-Profil einer bestimmten Polymerprobe stark beeinflusst. Es wurde eine neue optimale Fraktionierungsmethode für die CRYSTAF entwickelt, die zu qualitativ hochwertigen CRYSTAF-Profilen führt. Das Modellergebnis konnte durch die Anwendung der neuen Methode auf drei unterschiedliche Polyolefin-Blends experimentell bestätigt werden.

Contents

Chapter 1

Introduction

The chemical composition of semicrystalline polymers as heterogeneous materials is mainly defined by differences in chain length (molecular weight and its distribution), chemical composition of the different chains, the composition of the single chain itself (stereoregularity and branching) and by the specific phase structure with locally different crystallinity of the blend design.[1–3]

The material behaviour of polymer blends depends on the properties of the polymeric components, the phase morphology and the interaction between the phases.[4] The knowledge of these parameters is important to design new products with optimal material properties.[3–6] Nowadays polymer blends are of intensive scientific interest especially in the investigation of equilibrium and non equilibrium properties, in kinetics of phase transition and in further topics of statistical physics.[3–9]

As a consequence detailed polymer separation methods which give information about composition details are therefore highly relevant for a development of structure-properties-relations. Modern techniques for separating polymers according to their molecular size for determining the molecular weight distribution (MWD) are Size Exclusion Chromatography (SEC), Field Flow Fractionation (FFF) and Holtrup fractionation.[10–13] Investigating the polymer microstructure especially the chemical composition distribution (CCD) and the phase composition of semicrystalline polymer blends, Temperature Rising Elution Fractionation (TREF) and Crystallization Analysis Fractionation (CRYSTAF) are used as complementary separation techniques. The fractionation mechanism of TREF and CRYSTAF is based on intermolecular differences in chain crystallizabilities.[2,14–20]

TREF operates in two steps, the precipitation step and the elution step. In the precipitation step the low concentrated polymer solution is continuously cooled down in a column packed with an inert support. This process leads to a layer structure enclosing the support material, where the innermost layer represents a polymer fraction with high crystallizability contrary to the outermost layer which stands for a fraction with less crystallizability. In the second step temperature increases continuously, during which the solvent is pumped through the column. The solvent flow dissolves the layer structure in reverse order and transports the dissolved polymer fraction to an infrared (IR) detector, which detects on-line the polymer concentration at the specific elution temperatures.

This measurement leads to a TREF-profile representing the detector response versus elution temperature.[2,15,21]

An alternative time saving analysis technique to TREF is provided by CRYSTAF, which derives a separation profile from a sample in only one precipitation step. Herein the dissolved polymer is stirred in a vessel, while the temperature of the oven decreases continuously and the polymer precipitates stepwise. The respective concentration of the remaining polymer solution is measured by an IR-detector during the cooling process. The detector signal presents a cumulative concentration curve versus cooling temperature. The first derivation of the cumulative concentration curve maps the typical CRYSTAF-profile, which is similar to the TREF-profile in most cases.[16,20] According to the low analysis time and the efficient phase separation of polymer blends, CRYSTAF has become a powerful method in microstructure characterisation of semicrystalline polymers, thus it makes it of high interest.[16,22]

Factors which influence the separation process by CRYSTAF are not only molecular parameters such as comonomer content, comonomer size, co-crystallization effects, molecular weight at low molecular masses but also the experimental conditions set to the respective measuring apparatus by the operator.[14,20,23] This could recently be shown by simulating the influence of the experimental operating conditions which are based on a crystallization kinetics model.[24–27]

The idea of the current study is to develop a sample independent statistic mathematical model which describes the quality of separation of polymer blends during CRYSTAF analyses. This methodology aims to determine the experimental factors which strongly influence the non-equilibrium separation process by coupling a mathematical model with an experimental analysis. The knowledge of the parameters with high influence on the fractionation should lead to a new CRYSTAF method with high quality in analysing semicrystalline polymers and polymer blends, via experimental-mathematical non-linear optimization.

Chapter 2

Modern concepts of polymer separation techniques

Temperature Rising Elution Fractionation (TREF) and Crystallization Analysis Fractionation (CRYSTAF) are modern techniques separating and characterizing semicrystalline polymers. The following chapter focuses on general aspects of TREF and CRYSTAF and describes some mentionable features of TREF and CRYSTAF published in the literature.

2.1 Theory of polymers in solution

A dilute solution can be defined as a mixture in which the mole fraction of the solvent is close to unity.[28] Solubility or crystallizability fractionation of polymers in solution is discussed theroretically on the basis of Flory-Huggins thermodynamic theory.[16,29–31] This theory indicates a melting-point depression by the presence of a solvent which is expressed in Equation (2.1).

$$\frac{1}{T_m} - \frac{1}{T_m^0} = \frac{R}{\Delta H_u}\frac{V_u}{V_1}\left(\nu_1 - \chi_1\nu_1^2\right) \tag{2.1}$$

T_m^0 is the melting temperature of the pure polymer, T_m represents the equilibrium melting temperature of the polymer-diluent mixtures, ΔH_u stands for the heat of fusion per polymer repeating unit, V_u and V_1 are the molar volumes of the polymer repeating unit and the diluent, ν_1 is the volume fraction of the diluent and χ_1 is the Flory-Huggins thermodynamic interaction paramter.[16] R is the well known ideal gas constant. Equation (2.2) is used for random copolymers, where T_m^0 is the melting temperature of the pure homopolymer (e.g. polypropylene), ΔH_u is the heat of fusion of the homopolymer repeating unit (e.g. propylene), and p stands for the molar fraction of the crystallizing unit (e.g. propylene).

$$\frac{1}{T_m} - \frac{1}{T_m^0} = -\frac{R}{\Delta H_u}\ln(p) \tag{2.2}$$

Equation (2.1) is identical to Equation (2.2) at very small concentrations of solvent. As a consequence, noncrystallizing comonomer units (e.g. comonomer), diluents and polymer-end-groups cause a melting-point depression when the concentration of each is low and do not enter into the crystal lattice. Equation (2.2) can be simplified by setting $p = (1 - N_2)$, where N_2 is the molar fraction of the noncrystallizing units and by using the simplification $\ln(1 - N_2) \cong -N_2$ Equation (2.3) comes out.[16]

$$\frac{1}{T_m} - \frac{1}{T_m^0} = \frac{R}{\Delta H_u} N_2 \tag{2.3}$$

Equation (2.3) shows the higher the molar fraction of the incorporated comonomer the stronger the depression of the melting-point T_m)

2.2 Temperature Rising Elution Fractionation (TREF)

2.2.1 Separation mechanism of TREF

TREF fractionates semicrystalline polymers according to their solubility-temperature relationship which is directly coherent with the chemical composition distribution. TREF fractionates semicrystalline polymers only and it is not applicable to amorphous polymers because TREF is sensitive to differences in polymer crystallinity or rather solubility.[15] Figure 2.1 illustrates a homopolymer chain of a high density polyethylene (HDPE) as well as the structure of a polypropylene. The HDPE in the upper part of Figure 2.1 has a high structural order contrary to the molecule below, where a hydrogen is substituted by another chemical group (R). As a consequence the molecule with the disrupted structural order will not crystallize with the other regular chains thus the crystallinity of the polymer will be lower than that of the regular one. Also polymers with differences in stereoregularity such as polypropylene show that those molecules representing isotacticity have a higher crystallinity and stiffness than atactic molecules. TREF uses these effects to fractionate polymer chains.[15]

TREF operation can be devided into two steps, namely precipitation and elution. First the polymer is dissolved in a good solvent and mixed with an inert support for example stainless steel, glas beads, silica gel, sea sand, chromosorb P etc.[15,21]

Commonly used solvents are trichlorobenzene (TCB), *o*-dichlorobenzene (ODCB), xylene or α-chloronaphthalene. Then the mixture is slowly cooled down to room temperature under well controlled conditions and the polymer precipitates. The most easily crystallizable fraction precipitates first and builds the innermost layer of the support. Fractions with least crystallinity precipitates last and build the outermost layers. In this sense a structure of peelings is produced during the elution step. Each peeling stands for a polymer fraction representing a specific crystallizability.[15,21] Not precipitated molecules remain in solution. In the first step the cooling rate plays a major role for the fractionation quality.[32] In the second step the polymer is eluted during temperature increases. The polymer in solution is removed as the first fraction. At lower

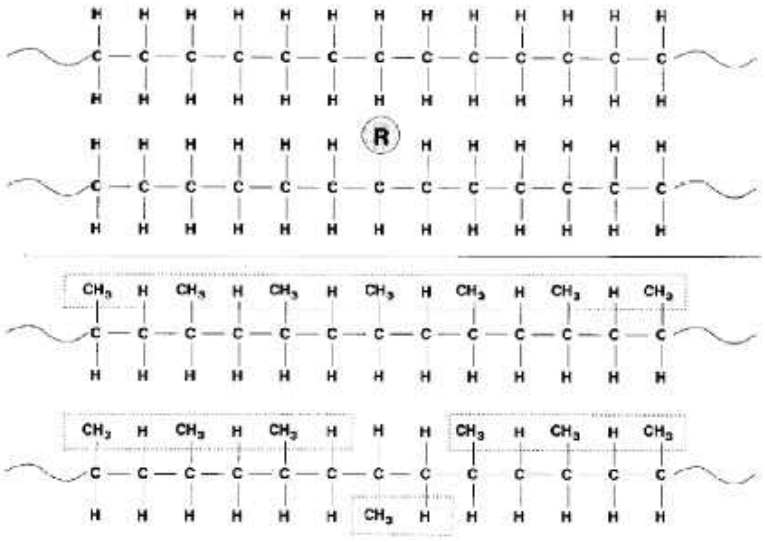

Fig. 2.1: Effect of comonomers in a chain structure of polyethylene and changes in stereoregularity of polypropylene (see text).[15]

temperatures fractions with less crystallizability, the outermost layers, are dissolved. With increasing temperatures fractions with higher crystallizability can be eluted.[15,21] The schematic separation mechanism can be seen in Figure 2.2.

TREF can be operated in preparative or analytical way. Preparative TREF (pTREF) separates polymer fractions at predefined temperature intervals and collects the fractions. This method is mainly used if extensive post-analysis for example determining the microstructure by NMR is required. Often preparative TREF is named off-line investigation.

Analytical TREF monitors the eluted polymer continuously by an on-line detector i.e. by connecting the column to a mass concentration detector. Table 2.1 makes a comparison of pTREF and aTREF in major aspects and gives a short schema of remarkable differences. The result of analytical TREF (aTREF) is the elugram which delivers detector response versus temperature. Using a calibration curve elution temperature can be related to the specific investigation property, short chain branching or molar mass for example.[14,15,21] In literature fractionation mechanism of TREF is basically explained by chain crystallizability. However few studies dealing with theoretical aspects, experimental limitations and additonal influences are published.[14]

2.2.2 Experimental limitations

Effect of molecular weight

It was exhibited that low molecular weight of a linear polyethylene with a narrow molecular weight distribution (MWD) shows a lower separation temperature than linear polyethylene in a higher molecular weight range. Experiments could verify that

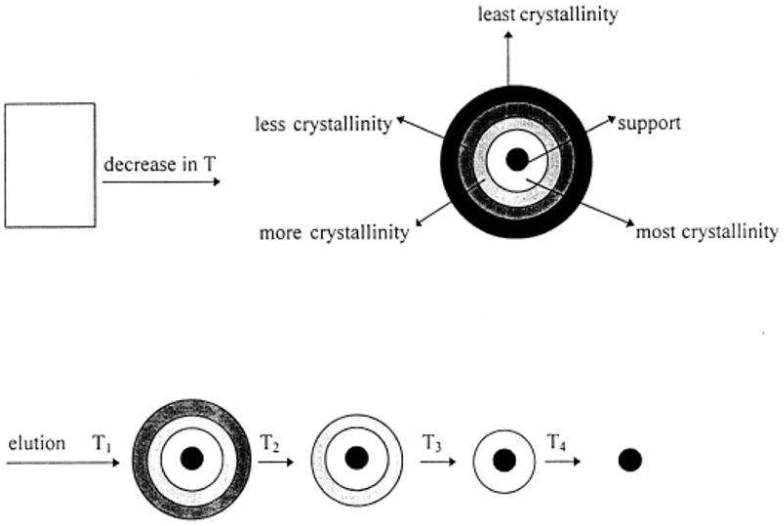

Fig. 2.2: Schematic separation mechanism of TREF.[21]

Tab. 2.1: Comparison of Preparative TREF and Analytical TREF[15]

preparative TREF (pTREF)	analytical TREF (aTREF)
Fractions are collected at predetermined temperature intervals.	Continuous operation
Information about molecular structure is obtained off-line by additional analytical techniques	Information about molecular structure is obtained on-line by means of calibration curve
Requires larger columns and larger sample sizes	Requires smaller columns and smaller sample sizes
Time-consuming but can generate detailed information about polymer microstructure	Faster than preparative TREF but generates less information about polymer microstructure

molecular weight should be higher than 10^4 for getting molecular weight independent TREF-profiles.[14,15]

Effect of comonomer size

Also comonomer size influences the separation mechanism. In melt crystallized fractions the melting points of the comonomer fractions with the longer branch length are lower than those fractions with shorter branches. Bulkiness influences the melting point as well as the degree of crystallinity. Melting points of fractions with the same comonomer content follows the order $octene-1 = 4-methylpentene-1 < hexene-1 < butene-1$. This effect leads to differences in comonomer- and SCB-distribution determined by using a TREF system with calibration curves.[14]

Effect of co-crystallization

Wild et al. investigated the short chain branching distribution (SCBD) obtained by TREF of a three blend system and compared it with the TREF-profiles of the individual fractions or rather the pure components of the blend. The three chosen samples were a linear polyethylene fraction, a high pressure low density polyethylene with a methyl content of 6.2 $CH_3/1000C$ and a high pressure low density polyethylene with a methyl content of 19.1 $CH_3/1000C$. They observed that the differences in the fractionation results were negligible. These authors adviced that co-crystallization in TREF is not really mentionable.[2]

Effect of packed column

Crystallization by TREF takes place in column and is influenced through an nucleation process and therefore, depends on the environment in which crystallization occurs. Perhaps the column packing material plays a major role in the TREF separation process. However, there are no extensive studies according to this topic.[14]

2.2.3 Application of TREF

Polyethylene

TREF is used to determine short chain branching (SCB) of low density polyethylene and whose relationship to polymerization conditions. In the high pressure process the level of SCB rises with increasing reactor temperature and decreasing reactor pressure. Long chain branching can be controlled by temperature and pressure too. Variation of reactor configurations and condition will vary SCBD of low density polyethylene. Also complex branch structures arising during the high pressure polymerization of ethylene was investigated by using TREF.[14] In this study it was noted that only a linear low density polyethylene represents the linear relationship between TREF elution temperature and methyl content. For low density polyethylenes with complex branch structures the

common linear calibration curve could not describe the relation, a non linear relation arises.[14]

Referring to linear low density polyethylene TREF delivers the characteristic broad and often bimodal intermolecular comonomer distribution regardless to the used catalyst system. Getting detailed information of the structure- property relationship it is necessary to investigate in which molecular weight species the comonomer is concentrated. For understanding the structure of linear low density polyethylenes the development of TREF was quite useful.[14]

Polypropylene

Contrary to polyethylene the crystallization process of polypropylene is initiated by a heterogeneous nucleation.[14]

Important structural properties of polypropylene is stereoregularity,i.e. isotacticity of the chain. Isotactic parts of the chain form helices only and crystallize in a lamellar arrangement. Tacticity distribution and stereodefects influence the crystallization behaviour and the thermomechanical properties of the polymer strongly.[33] Heterogeneous Ziegler-Natta-catalysts contain multiple active sites and produce polypropylenes with varying degree of stereoregularity.[34]

TREF separation is dependent on the stereoregularity along the chain and is potentially influenced by the nature of the catalyst, the polymerization conditions and if comonomers are used also by the comonomer type. According to this information TREF is used for characterizing the tacticity distribution of polypropylenes.[14]

2.3 Crystallization Analysis Fractionation (CRYSTAF)

2.3.1 Separation mechanism of CRYSTAF

CRYSTAF as well as TREF fractionates on the basis of crystallizability and by a slow cooling of the polymer solution.[35] In CRYSTAF the analysis is performed in a single step against to TREF where the process runs in two steps. According to the one analysis cycle (crystallization) CRYSTAF is a faster characterization method than TREF and it has lower hardware requirements. In CRYSTAF the analysis is carried out by monitoring the polymer solution concentration during crystallization by temperature reduction. Aliquots of the solution are filtered out of the vessel and analyzed by a concentration detector. In this approach the focus lies on the polymer which remains in solution.[35] Figure 2.3 shows a simplified schema of CRYSTAF fractionation technique.

The first data points, where no precipitation has happened, provide a constant concentration equal to the initial polymer solution concentration. When the cooling starts and the temperature goes down, the most crystalline fractions precipitate first and the concentration of polymer in the solution decreases. The result of the measuring process is a cumulative concentration curve. The first derivation of the cumulative curve rep-

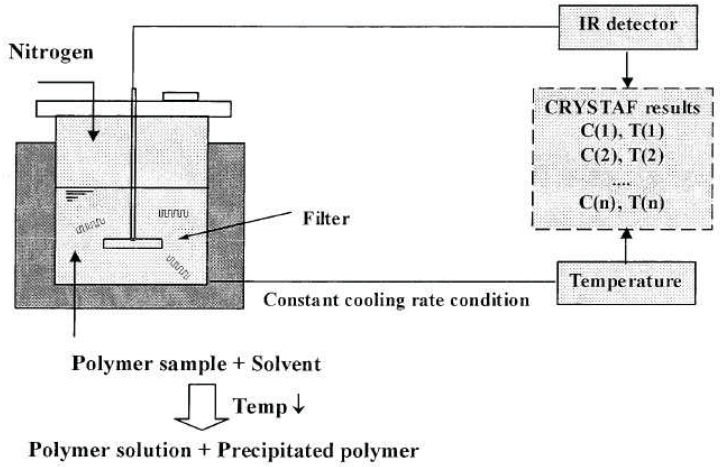

Fig. 2.3: Schematic principles of CRYSTAF fractionation.[23]

resents the typical CRYSTAF-profile and could be transformed by a calibration curve into a short chain branching distribution. Figure 2.4 shows these curves. The upper curve in Figure 2.4 is the cumulative curve or rather the cumulative SCBD if the temperature scale is calibrated and transformed to the number of branches/1000C which is explained in paragraph 2.3.2. The first derivation of the cumulative SCBD leads to the well known SCBD as it is shown in Figure 2.4.[16] It is remarkable, that the whole fractionation process occurs in a stirred vessel,contrary to TREF no column is required.

With this approach semicrystalline polymers could be fractionated and for example SCBD could be determined in only one crystallization cycle without physical separation of the fractions. The term Crystallization Analysis Fractionation (CRYSTAF) stands for this process. Preparative CRYSTAF is used to obtain a large amount of polymer fractions, which could be analyzed off-line.[35]

2.3.2 Calibration of CRYSTAF

CRYSTAF should be calibrated with polymer standards representing a narrow chemical composition distribution (CCD) and various average comonomer contents. The CRYSTAF-profile delivers the peak temperature of each standard. These temperature values are compared with the number of branches/1000C and a relation between the temperature scale and the short chain branching distribution could be obtained. Two methods exist for preparing the calibration curve which differ in the type of standard. One standard is synthesized with single-site catalysts, and the other standard is produced by preparative TREF fractions from broad-CCD Ziegler-Natta copolymers. It exists no universal calibration curve for CRYSTAF, this makes it necessary to prove that the unknown polymer investigated by CRYSTAF is nearly similar to the standards used for calibration.[20]

Calibration curves strongly depend on solvent type, cooling rate and method of

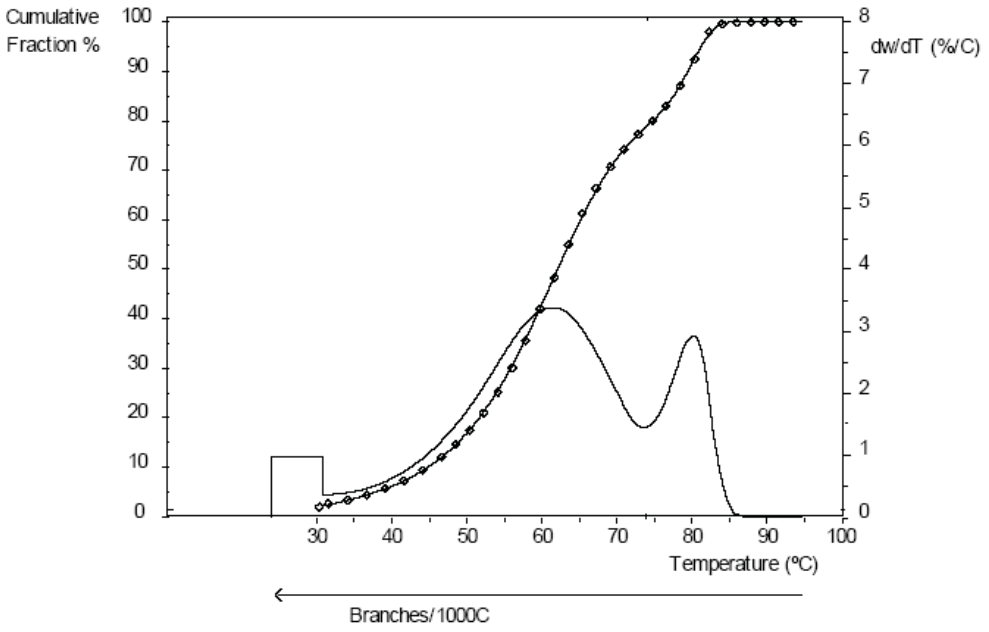

Fig. 2.4: Cumulative and differential SCBD of a linear low density polyethylene PE-LLD obtained by CRYSTAF.[35]

sample preparation.[20] This makes it necessary that samples of unknown CCD must be analyzed at the same conditions where the calibration curve is obtained. Recently a new methodology for constructing CRYSTAF calibration curves computationally by using a crystallization kinetics model for CRYSTAF was published by S.Anantawaraskul.[24] The simulated calibration curves are close to the experimental curves, and also the estimated CCDs with these calibration curves agree with the theoretical prediction from Stockmayer's bivariate distribution. In this study the cooling rate is the key operating condition influencing CRYSTAF-profiles and calibration curves mostly. Also the effect of molecular weight and the effect of comonomer type, quantified by the value of the longest ethylene sequence (LES), on calibration curves and CRYSTAF-profiles is quantified by S.Anantawaraskul.[23,24]

2.3.3 Experimental limitations

Effect of molecular weight

Crystallization temperature depends not significantly on molecular weight only below a number average molecular weight M_n of 5000 molecular weight affects CRYSTAF peak temperature. This result was obtained by an investigation of ethylene homopolymers with different molecular weights.[20] CRYSTAF-profiles of fractions of ethylene/1-hexene copolymers with different number average values of molecular weight show only a weak dependence of crystallization temperature but present strong differences in peak broad-

ness. CRYSTAF-profiles of polyethylene resins get broader with decreasing the number average molecular weight, as Figure 2.5 presents. Figure 2.6 shows the effect of molecular weight on CRYSTAF calibration curves for ethylene/1-hexene copolymers simulated at a cooling rate of 0.1 °C/min.[24]

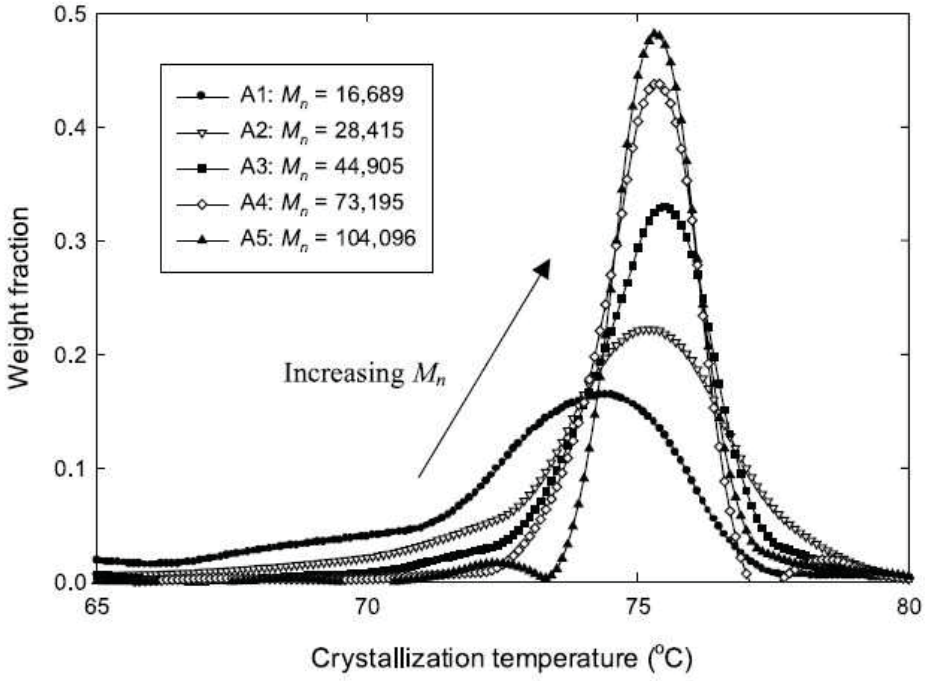

Fig. 2.5: Effect of molecular weight on CRYSTAF-profiles.[36]

Effect of comonomer content

Comonomer content affects the chain crystallizability and crystallization temperature of polyolefins mostly. Each comonomer stands for a defect in the regular chain and is responsible for lowering crystallizability. Figure 2.7 presents the CRYSTAF-profiles of a ethylene/1-hexene copolymer with nearly the same molecular weight and remarkable differences in comonomer content. Small differences in comonomer content are responsible for extreme peak shifts in CRYSTAF-profiles. Also the peak broad changes according to the comonomer content.[20]

Effect of comonomer size

An investigation of melting and crystallization behaviour of random propene/α-olefin copolymers by using differential scanning calorimetry (DSC) and CRYSTAF shows that melting temperature and crystallization temperature are independent of comonomer type.[37] Contrary to this result S.Filho[38] published that an ethylen/1-butene copolymer

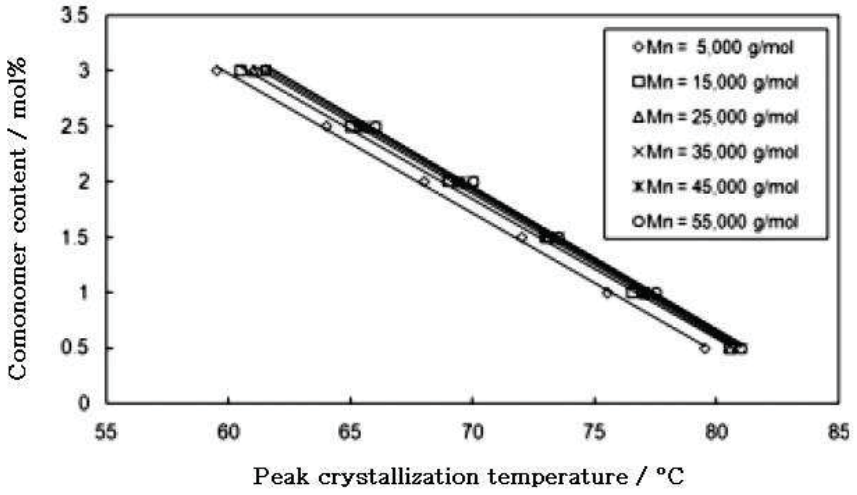

Fig. 2.6: Effect of molecular weight on CRYSTAF calibration curves.[24]

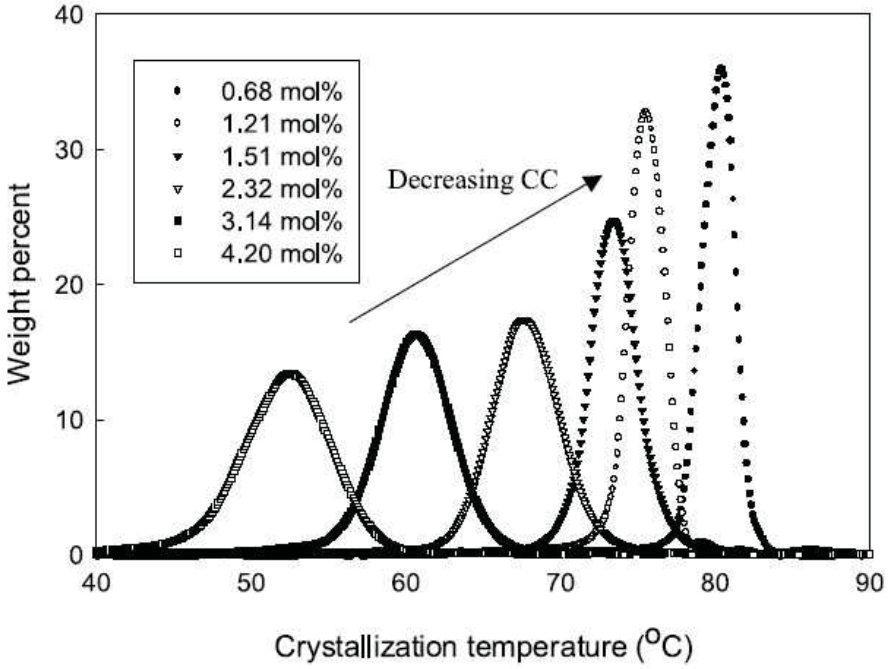

Fig. 2.7: Effect of comonomer content of CRYSTAF-profiles.[36]

and an ethylene/1-octene copolymer analyzed by CRYSTAF show different crystallization temperatures. It seems that CRYSTAF peak temperature for propene/α-olefin copolymers are independent of comonomer type when the comonomers are longer than 1-octene. For shorter comonomer types than 1-octene the crystallization temperature depends on comonomer type.[20]

Figure 2.8 shows the effect of comonomer type on CRYSTAF calibration curves for ethylene/1-hexene copolymers simulated at a cooling rate of 0.1 °C/min.[24]

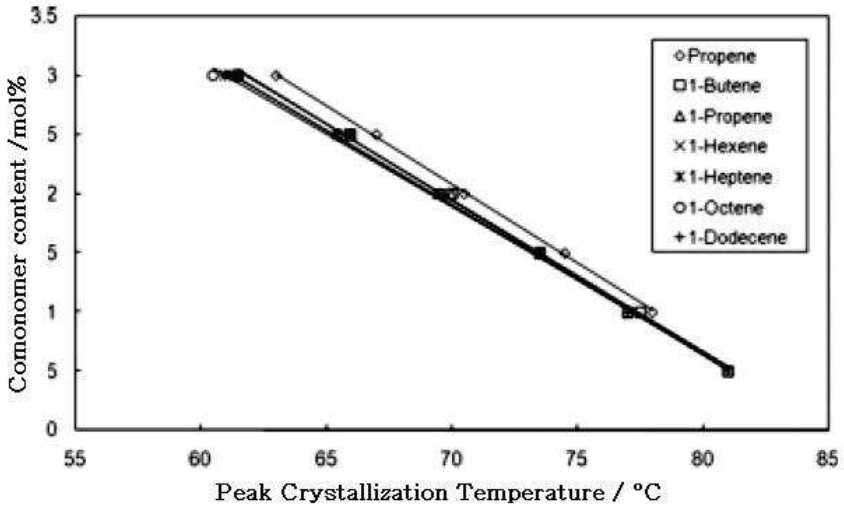

Fig. 2.8: Effect of comonomer content on CRYSTAF calibration curves.[24]

Effect of co-crystallization

Co-crystallization is the phenomenon where chains of different crystallizabilities crystallize at the same temperature. Referring to ethylene/1-olefin copolymers, co-crystallization leads to a simultaneous crystallization of chains with different 1-olefin-contents. This effect is really undesirable because it makes it impossible determining the CCD of the copolymers.[23]

Co-crystallization effects during CRYSTAF analysis can be studied by comparing the CRYSTAF-profile of a polymer blend with the weighted superposed CRYSTAF-profiles of the pure blend components which stands for the predicted CRYSTAF-profile without any co-crystallization. When the blend is made of polymers with different crystallizabilities, co-crystallization have not a significant effect on CRYSTAF-curves. However the crystallizabilities of the blend components are similar, the CRYSTAF-profile delivers one peak or rather a peak overlapping. Finally cooling rate and similarity of chain crystallizabilities affecting co-crystallization.[20]

2.3.4 Effects of the operating conditions on CRYSTAF

Effect of polymer concentration

The crystallization temperature of polymer solutions depends on their concentration. According to the fractionation process of CRYSTAF the concentration of the polymer in solution decreasis during the polymer precipitation. To prove that changes in polymer concentration are not affecting CRYSTAF analysis S.Anantawaraskul[23] investigated various polymer solutions with concentrations varying from 0.2 to 1.0 mg/mL at a constant cooling rate of 0.1 °C/min. Figure 2.9 shows the effect of the polymer concentration on CRYSTAF-profiles, as sample a ethylene/1-hexene copolymer with a M_n of 34.300 g/mol was used. It is documented by this study that a change of concentration in this range does not affect the results of CRYSTAF.[23]

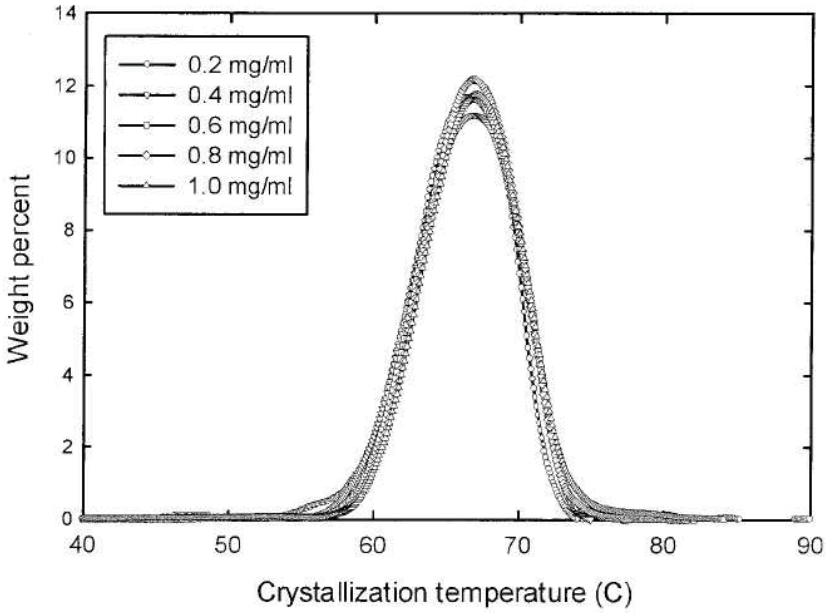

Fig. 2.9: Effect of the polymer concentration on CRYSTAF-profiles. (As sample a ethylene/1-hexene copolymer was used).[23]

The small differences between the CRYSTAF-curves in Figure 2.9 can be traced back to experimental measuring error of CRYSTAF and in this case they are not significant.

Temperature lag during analysis

The crystallization temperature denoted in the CRYSTAF-profile is measured in the oven room of the CRYSTAF apparatus. It was noted that CRYSTAF runnig with fast cooling rates represents differences between the measured oven temperature and the temperature in the vessel, this phenomenon is called temperature lag. Figure 2.10

shows the temperature lag as a function of CRYSTAF measuring temperature for various cooling rates.[23]

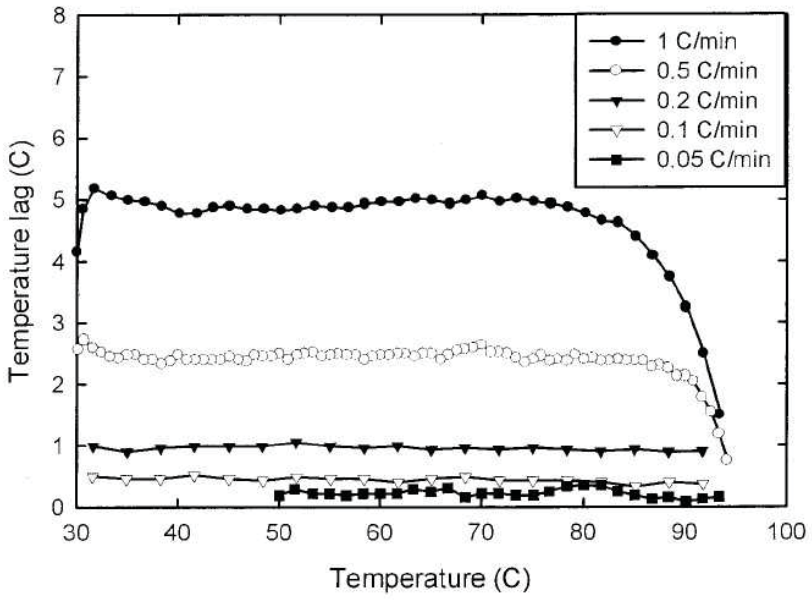

Fig. 2.10: Temperature lag between the oven temperature and the temperature inside the vessel at various cooling rates.[23]

It can be seen that in the temperature range of 30-85 °C there is a constant trend of the curves. Above 85 °C the curves decrease because the polymer used in this investigation starts precipitation at 85 °C. This makes it clear that the curves can be interpreted in a temperature range lower than 85 °C only. As a result the temperature lag for different cooling rates is constant versus CRYSTAF measuring temperature. Figure 2.11 shows the average temperature lag as a function of the cooling rate, which delivers a linear relation ship.[23]

The linear dependence reflects in the value of the squared coefficient of correlation r^2, which is 0.9998. The calculated linear equation can be seen in Figure 2.11, TL stands for temperature lag and CR stands for cooling rate. The linear equation is only a qualitative result, because it shows the linear dependence of temperature lag on cooling rate clearly and denotes that slow cooling rates lead to not mentionable temperature lags. It could not be used for determining the quantitative temperature lag for other CRYSTAF apparatus, because it relates to the CRYSTAF appartus used for this study only.[23]

Effect of cooling rate

Figure 2.12 and 2.13 show the effect of the cooling rate on the integral and derivative CRYSTAF-profiles. The sample which was used for this analysis is a ethylene/1-hexene

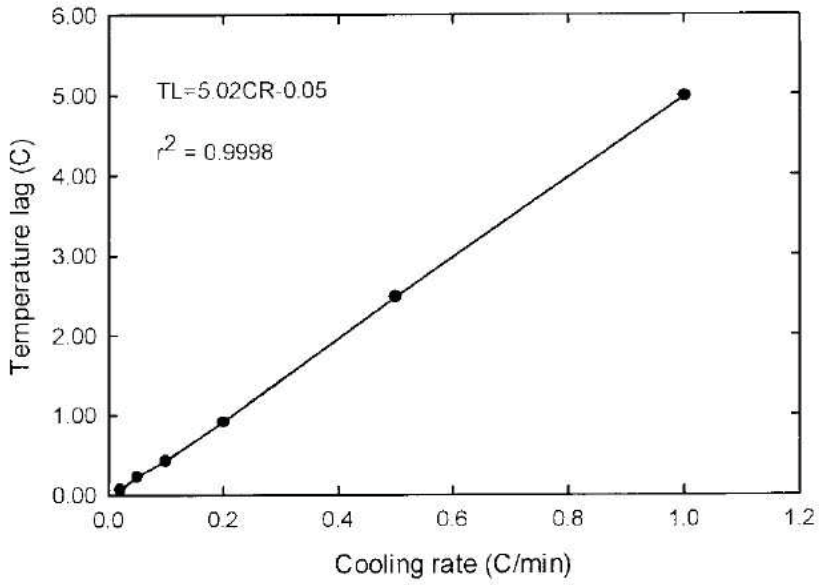

Fig. 2.11: Average temperature lag as a function of the cooling rate.[23]

copolymer with a M_n of 36.300 g/mol. These studies present clearly that slow cooling rates lead to crystallization temperature peaks at higher temperatures. The profiles were corrected to account for the temperature lag in the system.

It is interesting that the typically used cooling rate of 0.1 °C/min is in the middle of the derivative curves in Figure 2.13, this denotes that the typical cooling rate of CRYSTAF is far away from the therodynamical equilibrium. The CRYSTAF-profile shape changes likley if cooling rate goes to very slow cooling rates. This effect can be explained by the degradation and/or crosslinking of the polymer during the analysis process of CRYSTAF, because at very slow cooling rates, given in Figure 2.13, analysis time is about of two weeks.[23]

Between the CRYSTAF peak temperature T_P and the natural logarithm of the cooling rate exists a linear relationship, shown in Figure 2.14. The general empirical linear relationship can be seen in Equation (2.4).

$$T_P = a \cdot ln(CR) + b \tag{2.4}$$

In Equation (2.4) T_P stands for crystallization peak temperature, CR is cooling rate and a and b are sample typical parameters. These parameters depend on the average comonomer content of the sample. This is also the reason making calibration curves dependent on cooling rate.

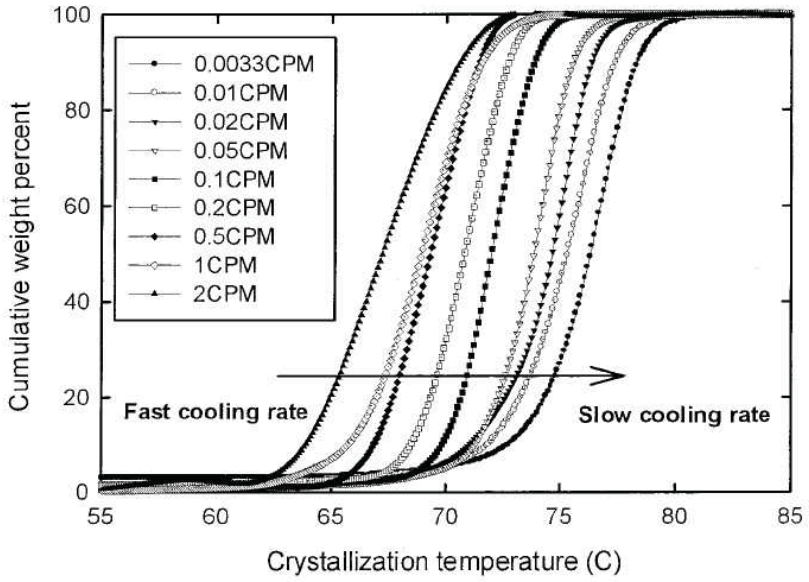

Fig. 2.12: Integral CRYSTAF curves of a ethylene/1-hexene copolymer at various cooling rates.[23]

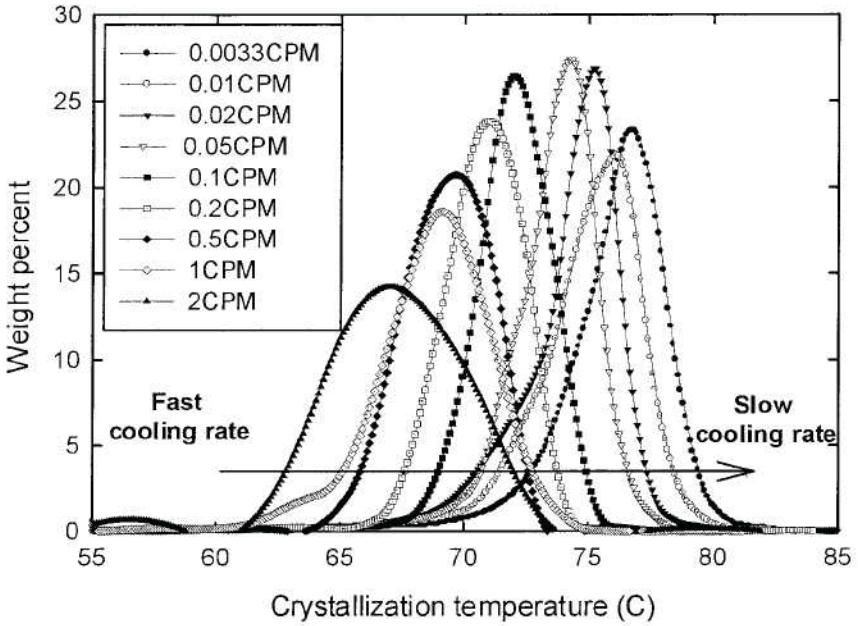

Fig. 2.13: Derivative CRYSTAF curves of a ethylene/1-hexene copolymer at various cooling rates[23]

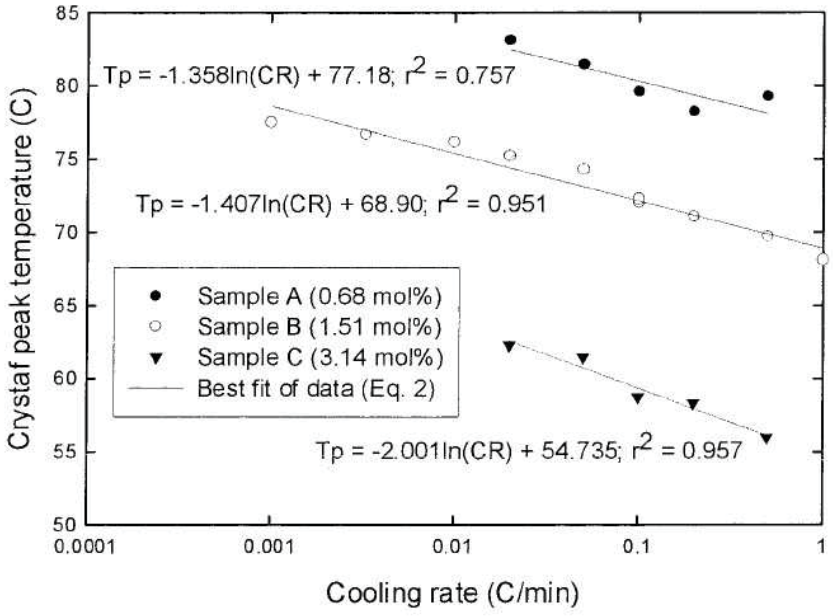

Fig. 2.14: CRYSTAF peak temperature as a function of cooling rate for ethylene/1-hexene copolmers with different comonomer content [23]

2.3.5 Application of CRYSTAF

A main application of CRYSTAF is analyzing CCD of semicrystalline polymers especially polyolefins. Based on calibration curves the comonomer content of samples like linear low density polythylene can be determined. CCD's are interesting for the specific design of structure property relation ships and deliver important information for polymer reaction engineering. It can be used to identify the nature of active site types in Ziegler-Natta catalysts. Contrary to TREF, CRYSTAF is a more timesaving method. It is also used to provide important insight into polymerization conditions which affect the polymer CCD. More understanding leads to targeted manipulation of CCD to obtain copolymers with specific microstructures through the combination of catalysts, co-catalyst, and support treatments. [20]

CRYSTAF is also deployed in the area of degradation, for example monitoring the changes in the chemical heterogeneity during thermooxidative degradation of polypropylenes. Recently CRYSTAF is also applied in blend analysis. [20]

Chapter 3

Experimental

The following chapter describes the characterization techniques and experimental conditions as well as the materials used in this study. All methods are state of the art in polymer characterization and are composed by using recent literatur and cooperate with leading companies producing polymer characterization instruments.

3.1 Experimental conditions of TREF

3.1.1 Apparatus and solvent

As TREF apparatus the TREF200 system from Polymer Char S.A. (Valencia,Spain) equipped with a linear response infrared detector, (measuring a wavelength around 3.5 μm) was used. The detector monitors the absorption of the C-H bonding of the eluted polymer.

As solvent and eluent 1,2,4-Trichlorobenzol (TCB, $\geq$ 99.0%) (Acros Organics, Geel, Belgium) containing 0.03% (w/v) 2,6-di-tert-butyl-4-methylphenol (BHT $\geq$ 98.0%) (Fluka, Buchs, Switzerland) was used. All polymers available in granular form are cut into pieces to assure a good dissolution of the polymer prior to TREF analysis starts.[32]

3.1.2 Analytical method

The specific analysis parameters are listed in Table 3.1 according to the study of N.Aust et.al.[32] The most dominating operating conditions of TREF are cooling rate (°C/min), heating rate (°C/min), start stablization temperature (°C) and elution rate (mL/min). The filling volume of each vessel amounts to 20.00 mL and the column load volume is set to 1.60 mL. The pump flow amounts to 0.50 mL/min. The concentration of the polymer solution averages 0.2% (w/v). The most important parameters to set are summarized in Table 3.1. The complete analysis is subdivided in six steps:

- Dissolution of the polymer (abbreviated Diss.)
- Start stabilization temperature of the polymer solution (abbreviated Stab.I)

- Cooling cycle with the specific cooling rate (abbreviated Cool.)
- Stabilization temperature before elution step starts (abbreviated Stab.II)
- Elution of the precipitated polymer (abbreviated Elu.)
- Cleaning cycle of each vessel (abbreviated Clean.)

Tab. 3.1: Conditions of aTREF Temperature Profile (Maximum Temperature: 171 °C, Top Oven Temperature 150 °C, Low Stirring: Continuous Mode (c), High Stirring: Discontinuous Mode (d)

	diss.	stab. I	cool.	stab. II	elu.	clean.
rate/ (°C/min)	40.0	-	0.20	-	1.00	-
temp./ (°C)	160.0	95.0	95.0-40.0	40.0	40.0-140.0	160.0
stirring/ (rpm)	200.0 (d)	200.0 (d)	100.0 (c)	100.0 (c)	100.0 (c)	200.0 (d)

3.2 Experimental conditions of CRYSTAF

3.2.1 Apparatus and solvent

As CRYSTAF apparatus the converted TREF200 system from Polymer Char S.A. (Valencia,Spain) equipped with a linear response infrared (IR) detector was used. The measuring wavelength of 3.5 μm monitors the absorption of the C-H bonding of the polymer. As solvent 1,2,4-Trichlorobenzol (TCB, $\geq$ 99.0%) (Acros Organics, Geel, Belgium) containing 0.03% (w/v) 2,6-di-tert-butyl-4-methylphenol (BHT $\geq$ 98.0%) (Fluka, Buchs, Switzerland) was used. The granulate polymer material was cut into small pieces to assure an easy solubility prior to CRYSTAF analysis. During the cooling cycle 34 samples of each polymer solution were pumped to the IR detector resulting in a CRYSTAF cumulative curve constructed from 34 supporting points. Each of the 34 samples were left for 20 s in the detector before the sampling time of 30 s started. The vessel pressure during analysis was 2 bar, the concentration of each polymer solution prepared was 1 mg/mL.

Configuration of CRYSTAF hardware

Contrary to the software configuration of CRYSTAF the hardware configuration is more time consuming. The change from analytical temperature rising elution fractionation (aTREF) to analytical crystallization analysis fractionation (aCRYSTAF) can be explained in six steps. The configuration is visualized in Figure 3.1. The symbols in Figure 3.1 are related to the configuration steps below.

- First of all the waste line 3 should be removed from the Valco connector. The Valco connector remains connected to the line coming from the IR-detector.
- Further the line from position 1 of 4PV (PV stands for port valve) must be disconnected and should be placed into the Valco connector (1).
- Next the line from position 6 of 6PV is placed into position 1 of 4PV (2).
- A cup is put into position 6 of 6PV.
- Further the union line between 4PV and 6PV is removed from position 4 of 4PV (3). The line is plugged with a cup.
- Waste line 3 removed at the first step goes now to position 4 of 4PV (4).

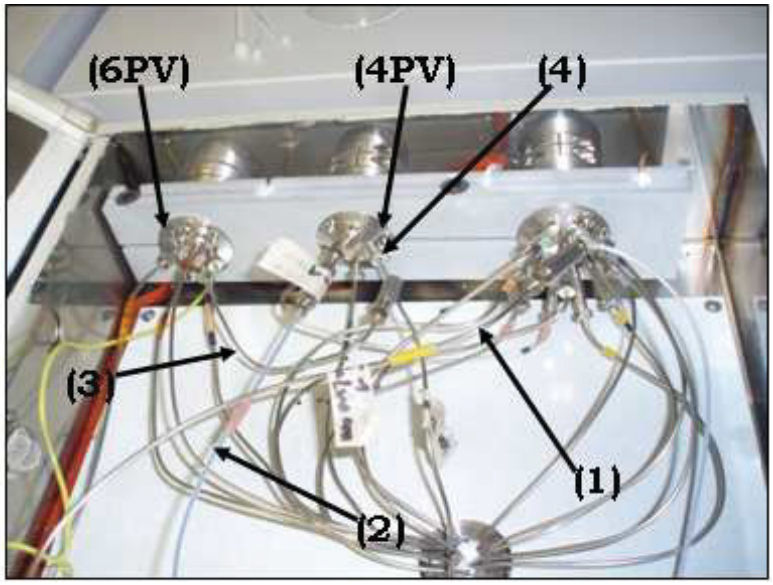

Fig. 3.1: Hardware configuration of CRYSTAF.

The hardware configuration steps are modified from TREF user manual.[39]

Configuration of CRYSTAF software

All files which are used for converting software can be found on the installation CD from Polymer Char (Valencia,Spain).

Installing software the following steps must be done:

- Creating a folder named: C:/PolymerChar/Crystaf.
- The file base.mdb should be copied into this folder.

- Further the files CRYSTAF.exe and CRYSTAF.ini should be copied in the folder C:/PolymerChar.
- In the folder C:/PolymerChar/shared the file config.pmc should be renamed to configback.pmc.
- At least the new file config.pmc from CD (Polymer Char S.A.) should be copied into the folder C:/PolymerChar/shared.

CRYSTAF operation Test

After the equipment and software have been installed, a test procedure, where no nitrogen and solvent is required, should be carried out by choosing manual action and pressing all buttons in the Safety First Screen. Initialization occurs with initial movement of valves and dispenser. Then the proper operation of all controls must be checked in the manual control screen.[35] The following parameters have to be checked:

- top oven temperature (setting a temperature in °C)
- main oven temperature (setting a temperature in °C)
- detector (lamp should light when switched on and read outs should appear in the screen)
- dispenser (move syringe up and down with gar left buttons)
- Valco 2 way valve (pressing with the mouse on the valve drawing)
- Valco multiposition valves (pressing with the mouse on the valve drawing)
- Gas sensor (check reading and move red alarm line to appropriate setting)[35]

3.2.2 Analytical method

According to the CRYSTAF users manual[35] and in collaboration with Polymer Char S.A. (Valencia,Spain) a standard analysis method could be designed. The operating parameters of this method are illustrated in Tables 3.2, 3.3 and 5.1 (Chapter 5). The whole process is subdivided into dissolution, stabilization, analysis (cooling) and cleaning. Cooling rate represents the operating parameter with a remarkable influence on CRYSTAF-profiles.[23]

3.3 Materials

The investigations were carried out with three different polyolefin blends, each consisting of 80 % of a heterophasic polypropylene matrix (random polypropylene polyethylene copolymer, RACO) and 20 % of different polyolefin based modifiers as disperse phase. Both, RACO and modifier, have a similar viscosity behaviour to ensure a good

Tab. 3.2: Standard Conditions of aCRYSTAF Temperature Profile (Maximum Temperature: 171 °C, Top Oven Temperature 150 °C, Low Stirring: Continuous Mode (c), High Stirring: Discontinuous Mode (d)

	dissolution	stabilization	analysis	cleaning
rate/ (°C/min)	20.0	-	0.20	-
temp./ (°C)	160.0	95.0	95.0-30.0	160.0
stirring/ (rpm)	200.0 (d)	200.0 (d)	100.0 (c)	200.0 (d)

Tab. 3.3: Detailed Operating Conditions of aCRYSTAF (V.:Volume, Pick.s.: Pick up speed, Pump.s.: Pump speed, W.s.: Waste speed)

FILLING	V.:two steps	30 mL	Pick.s.:	40 mL/min	Pump.s.:	15 mL/min
ANALYSIS	Sample V.:	1.50 mL	Pick.s.:	8 mL/min	Pump.s.:	8 mL/min
	Returned V.:	1.50 mL	W.s.:	8 mL/min		
	Waste V.:	2.50 mL				
CLEANING	V.:	35 mL	Pick.s.:	40 mL/min	Pump.s.:	15 mL/min
	Cycle:	1				

compatibility during processing. As modifiers a C2C8-elastomer, a linear low density polyethylene (PE-LLD) and a high density polyethylene (PE-HD) were used. Sample codes and composition of the polymer blends are collected in Table 3.4. All blends were produced on a 16 mm Twin Screw compounder (PRISM TSE 16 TC, Thermo Fisher Scientific Inc., Waltham, MA, USA) at temperatures between 210-220°C. The mixtures are stabilized with 0.2 wt.-% of a commercially available stabilizer of the Irganox-type in order to prevent degradation.

Tab. 3.4: Sample Codes and Composition of the Polymer Blends Used in this Investigation

sample code	matrix polymer	modifier	wt.-% matrix	wt.-% modifier
Mixture 1	RACO	C2C8-elastomer	80	20
Mixture 2	RACO	PE-LLD	80	20
Mixture 3	RACO	PE-HD	80	20

The investigation of the polymer blend morphology was done by Borealis Polyolefine GmbH Linz by using Transmission Electron Microscope (TEM). The pictures were taken

from ultra thin samples that were formerly stained in an aqueous solution of ruthenium tetroxide. This leads to an observation of the amorphous phase by dark color.[40] Avoiding particle orientations the samples from which the slices (85 nm) were taken, were first prepared by melting them in vacuum at 200 °C in a press. The pictures were made with a CCD-Camera (Bioscan) from Gatan Inc.(Abingdon, UK). The TEM-analysis was done at the Institute for Electron Microscopy and Fine Structure Research (FELMI) in Graz. The picture were analysed with the image analysis software ImageJ.[41]

Figures 3.2, 3.3 and 3.4 show the morphology of Mixture 1, Mixture 2 and Mixture 3 with different scales. The multi-phase structure of the polymer blends can be observed. For all Mixtures the matrix is formed by the base polymer (RACO). The modifier can be seen in the form of inclusions. The connection of the matrix with the inclusions by PE-lamellae in the mixture is based on RACO and PE. If PE-HD is used as modifier PE-lamellae can also be found in the matrix. This can be interpreted as indication for partial miscibility of the two components.[41]

3.4 Statistical parameters of TREF- and CRYSTAF-profiles

Statistical parameters of TREF- and CRYSTAF-curves indicated mostly are weight average temperature T_W (Equation (3.1)), number average temperature T_N (Equation (3.2)), ratio r (Equation (3.3)) and σ as value for scattering broadness (Equation (3.4)).[39]

$$T_W = \frac{\sum T_i c_i}{\sum c_i} \tag{3.1}$$

$$T_N = \frac{\sum c_i}{\sum \frac{T_i}{c_i}} \tag{3.2}$$

$$T_W = \frac{T_W}{T_N} \tag{3.3}$$

$$\sigma = \sqrt{\frac{\sum c_i (T_i - T_W)^2}{\sum c_i}} \tag{3.4}$$

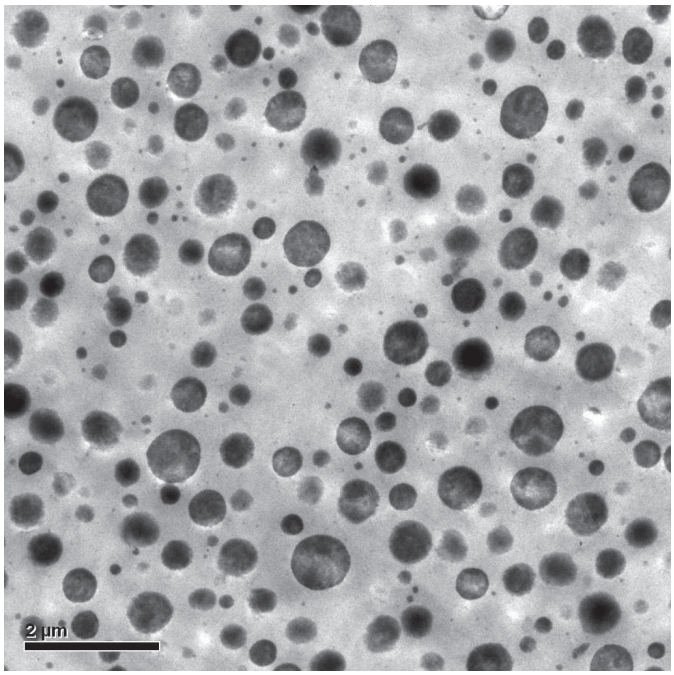

(a) scale: 2 microns

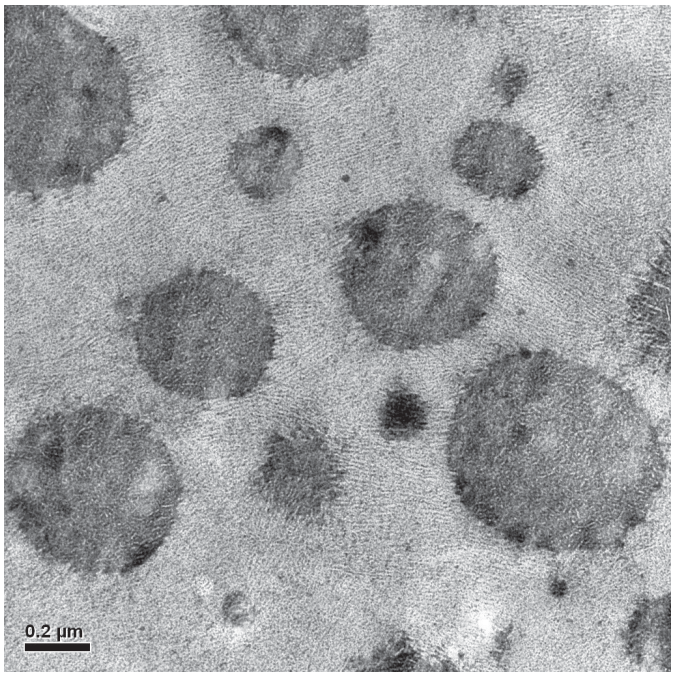

(b) scale: 0.2 microns

Fig. 3.2: TEM picture of Mixture 1; different scales.[41]

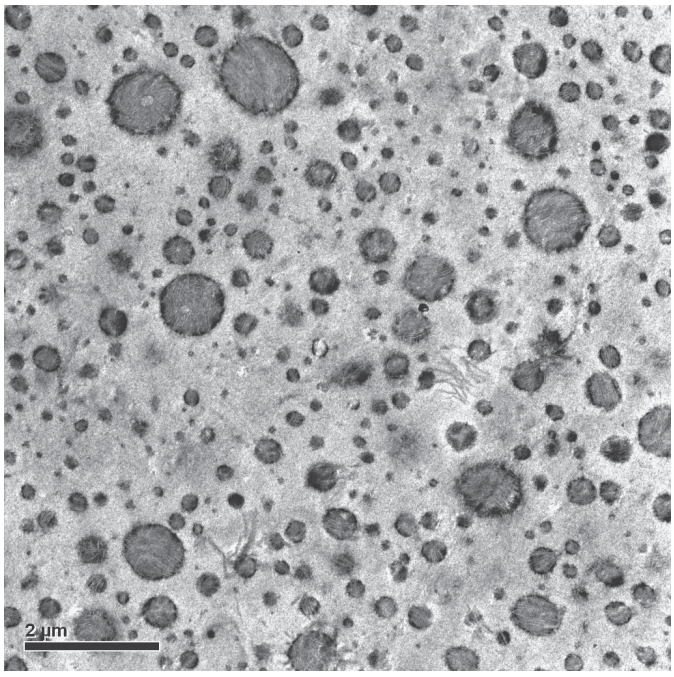

(a) scale: 2 microns

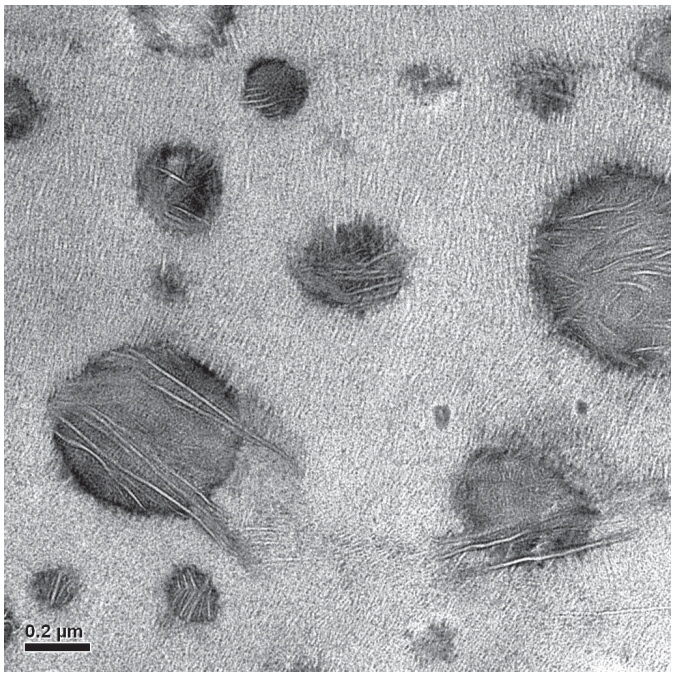

(b) scale: 0.2 microns

Fig. 3.3: TEM picture of Mixture 2; different scales.[41]

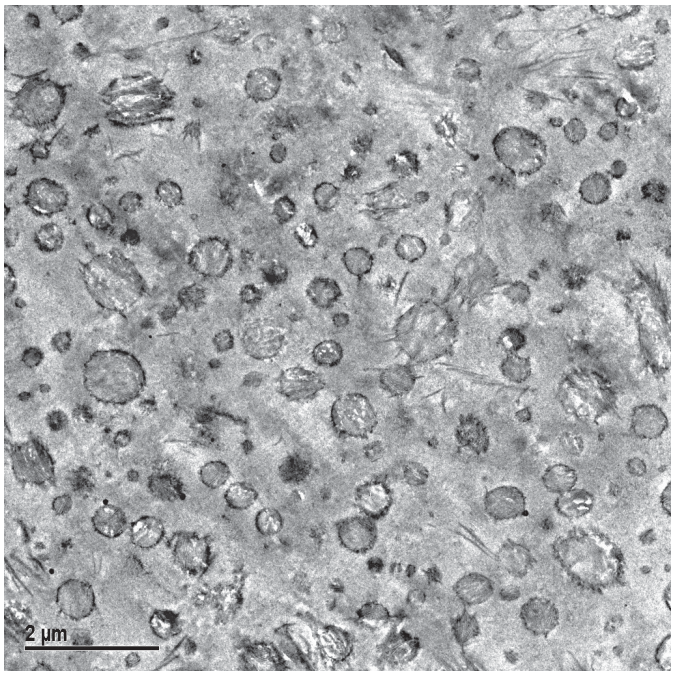

(a) scale: 2 microns

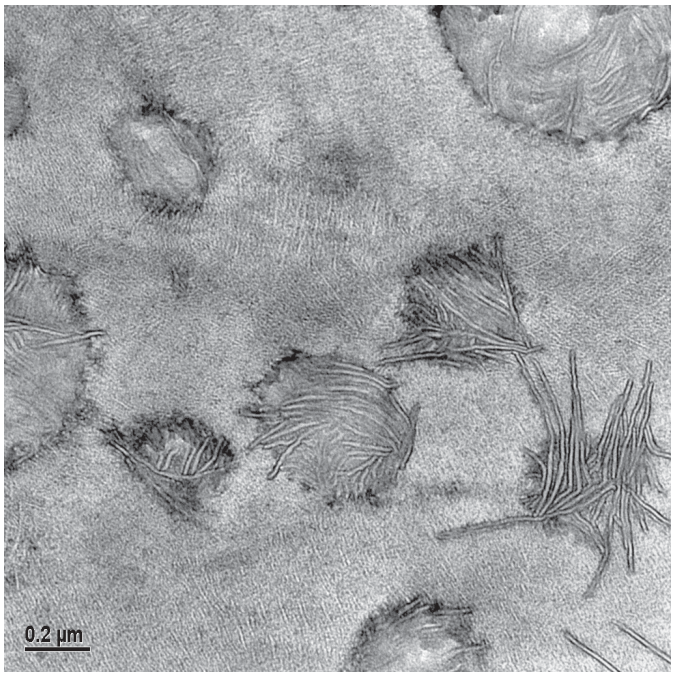

(b) scale: 0.2 microns

Fig. 3.4: TEM picture of Mixture 3; different scales.[41]

Chapter 4

Modeling of CRYSTAF curve quality and optimization

4.1 Modeling

Figure 4.1 schematically illustrates the structure of the CRYSTAF modeling system used in this investigation. Identification of the most important input parameter of the CRYSTAF apparatus, which stands for the "Real System" leads by abstraction to the abstract "Model System". This basic idea allows modeling of complex structure phenomena of reality and is derived from computer science.[42]

4.1.1 Definition of operating conditions

Parameters influencing the separation process are concentrated in the term "various operating conditions" (see Figure 4.1). CRYSTAF itself represents the "Real System". The "CRYSTAF curve", as a result of the experimental process, reflects the response of CRYSTAF depending on operating conditions and sample. As can be further seen from Figure 4.1, by building the "Abstraction" of the "Real System" the reduction of "various operating conditions" to a set of "selected operating conditions" is assumed.

This set mainly influences the CRYSTAF separation process. According to recent literature a significant operation parameter influencing CRYSTAF is the cooling rate.[23,24] Optimization analysis of TREF showed a dependency of the separation process on stabilization start temperature.[32] In TREF the dissolved polymer is separated in a column. Contrary to this the separation process in CRYSTAF occurs in a vessel, while the polymer solution moves circularly in a static acceleration field by a stirrer. Therefore, we assume that also stirring speed, which is an admeasurement for centripetal and accordingly centrifugal acceleration, may influence the polymer separation process in CRYSTAF. Due to this consideration a set of "selected operating conditions" with fixed intervals is the input of the abstract "Model System". This set is defined by cooling rate, stabilization start temperature and stirring speed.

The sample concentration is kept constant for each treatment at 1 mg/mL. Experi-

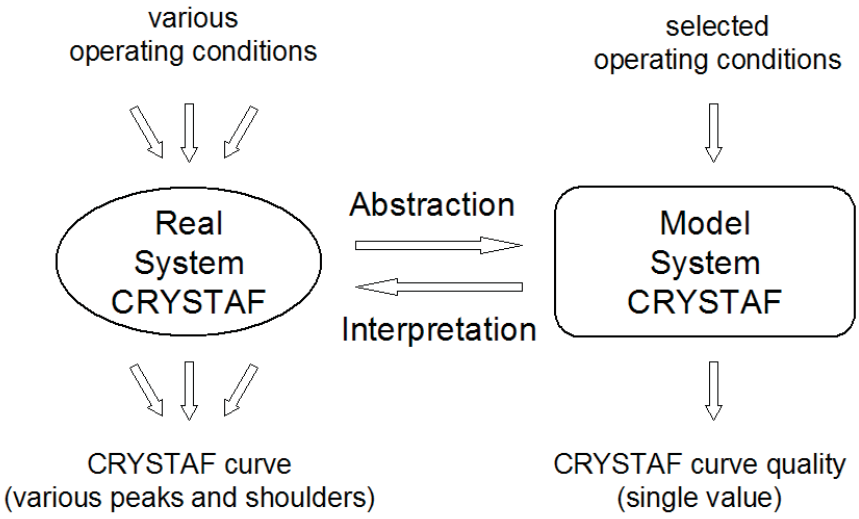

Fig. 4.1: Modified schematic modeling of CRYSTAF derived from complex structure modeling in computer science according to reference.[42]

ments show that the sample concentration does not influence the CRYSTAF profiles in the range between 0.2 - 1.0 mg/mL.[23]

4.1.2 Abstraction of the real system to the model

As abstraction model a randomized three factor two level factorial is used, which is a specific form of the general case of the three factor factorial. The factorial design is derived from literature.[43–45] Three factor factorials deliver a response in the general case of y_{ijkl} (see Equation (4.1)), when factor A is at the ith level ($i = 1, 2, ..., a$), factor B is at the jth level ($j = 1, 2, ..., b$) and factor C is at the kth level ($k = 1, 2, ..., c$) for the lth replicate ($l = 1, 2, ..., n$). For two levels $a = b = c = 2$. The high level of a factor is coded with $(+1)$ and the low level of every factor is coded with (-1). The codification of the factor quantities is reasonable for simplifying the calculation. In Equation (4.1) μ is the overall mean effect, τ_i represents the effect of the ith level of factor A, β_j is the effect of the jth level of factor B and γ_k is the effect of the kth level of factor C. These effects are also known as main effects. The terms $(\tau\beta)_{ij}$, $(\tau\gamma)_{ik}$, $(\beta\gamma)_{jk}$ and $(\tau\beta\gamma)_{ijk}$ are the effects of interaction, ϵ_{ijkl} is the random error component.

$$y_{ijkl} = \mu + \tau_i + \beta_j + \gamma_k + (\tau\beta)_{ij} + (\tau\gamma)_{ik} + (\beta\gamma)_{jk} + (\tau\beta\gamma)_{ijk} + \epsilon_{ijkl} \tag{4.1}$$

The application of an analysis of variance to the three factor model leads to the significance of each effect. It allows the determination of the response function of the factorial experiment with those factors influencing the response considerably. There have to be $n \geq 2$ replicates in order to calculate a sum of squares to determine if all chosen effects are significantly included in the model. Herein the three-factor analysis of variance model according to reference[43] is applied. The calculation of the sum of squares and the degrees of freedom for each effect and interaction yields the corresponding mean square. By dividing the mean square of the corresponding main effect or interaction by the mean square error, the test statistics F_0 of the specific effect is obtained. If $F_0 \geq F_{1-\alpha}$, where $1 - \alpha$ is the confidence interval, the effect is significant. In advance of calculating the response function of the factorial design, the output must be defined.

4.1.3 Definition of the output

Subsequently the significant response function of the factorial experiment can be obtained. Thus the design of the abstract model is the response function $\hat{y}$ where $\hat{y} : \Omega \rightarrow \Psi$ and $\Omega \subset \mathcal{R}^3, \Psi \subset \mathcal{R}$, which associates the three selected operating conditions in the predefined interval with the scalar quality value of the CRYSTAF profile (Equation (4.2)).

$$\hat{y} = f(x_1, x_2, x_3) \tag{4.2}$$

Ω is a closed connected region or rather a closed subset of the real set $\mathcal{R}^3$. The coefficients of the polynomial function of third order are calculated by bisection of the effects.[43–45] The variable x_1 stands for the coded variable of cooling rate, x_2 is the coded variable of stabilization start temperature and x_3 is the coded variable of stirring speed.

The definition of the scalar quality value for a CRYSTAF profile bears to the structure of the CRYSTAF curve. The higher the number of peaks and shoulders in a diagram of the same sample, the better the information of polymer fractions with differences in chemical composition, short chain branching, and phase structure is. The sum of the peaks weighted with 70 % and shoulders weighted with 30 % delivers an absolute quality value for each CRYSTAF curve. The data collection of each sample comprises 8 CRYSTAF profiles. By division of the absolute quality value of each CRYSTAF curve in the sample data collection through the highest absolute quality value, which was found for a CRYSTAF curve in this data collection, the relative quality value can be obtained. This approach delivers a sample independent definiton of quality which is the response of the model function.

4.1.4 Finding optimal operating conditions

Nonlinear optimization of the model function $\hat{y}$ leads to operating parameters within the fixed interval, which result in the highest quality of the CRYSTAF curve. Mathematically it is a constrained maximization problem of a nonlinear polynomial function (Equation (4.3)).[46]

$$max\ \hat{y} : \mathcal{R}^3 \rightarrow \mathcal{R} \text{ for } x \in \Omega \subset \mathcal{R}^3 \text{subject to constraint} \tag{4.3}$$

4.1.5 Experimental mathematical optimization of a nonlinar equation

To solve the maximization problem a specific method of experimental mathematics can be used. The idea of the solving method is the definition of a closed connected region defined by the three independent input variables x_1, x_2, and x_3. Each coordinate of the region can be reached by a specific modulation of the input variables. Simultaneously this modulation delivers a scalar quality value $\hat{y}$. Now a color bar which estimates a color gradient from low to high quality, where each $\hat{y} \in \Psi$ represents a specific color, is used as alternative to the mapping of the $\hat{y}$ in the fourth dimension. Therefore, a colored connected three dimensional region can be constructed. By systematically slicing the region Ω the color can be found which represents the highest quality value. In this way the optimal values for the operating conditions of CRYSTAF can be determined and applied to the CRYSTAF apparatus ("Interpretation", see Figure 4.1) which should lead to a CRYSTAF profile of highest quality which then can be compared to profiles derived at non optimized standard conditions.

4.2 Results

4.2.1 Simulation of the CRYSTAF curve quality depending on operating conditions

The 2^3 factorial design is performed experimentally in a random order, which is illustrated in Table 4.1. The variation of three different factors cooling rate (A), stabiliza-

tion start temperature (B) and stirring speed (C) leads to eight treatment combinations. Therefore, the three polyolefin blends are analysed by analytical CRYSTAF, where each blend was measured at 8 different operating condition modulations. The fixed interval ranges of the factors and their transformations in coded variables is shown in Table 4.2. The fixed intervals of the transformed variables define the closed set Ω.

Tab. 4.1: Nomenclature of the Randomly Ordered Factorial Design in this Study, 8 Treatment Combinations given in Coded Variables

random run	factor A	factor B	factor C	treatment combinations
7	-1	-1	-1	(1)
3	+1	-1	-1	a
8	-1	+1	-1	b
4	+1	+1	-1	ab
1	-1	-1	+1	c
6	+1	-1	+1	ac
5	-1	+1	+1	bc
2	+1	+1	+1	abc

Tab. 4.2: Defined Levels of the Factors and Transformation of the Factor Levels to Coded Variables

factor	factor quantity upper level	factor quantity lower level	coded variable upper level	coded variable lower level
cooling rate (A)	0.3 °C/min	0.1 °C/min	+1	-1
start crystallization temperature (B)	140 °C	95 °C	+1	-1
stirring speed (C)	150 rpm	50 rpm	+1	-1

In Table 4.3 the results of the relative quality determination for each sample and treatment combination are listed. The values are calculated as described in paragraph "Modeling". The relative total quality value is the sum of the quality values of each single mixture for a certain run. As can be seen in Figure 4.2 the relative quality values show a satisfying tendency of quality versus the different treatment combinations, with only limited scattering in the high quality region. This result shows the independence of the quality definition of a certain sample. Furthermore, it allows the argumentation that the abstracted "Model System" created is almost sample independent as well.

With the input ranges, the factorial design and the defined output values, the main

Tab. 4.3: Relative Quality Values (r.q.v.) Obtained for each Treatment Combination

Random Run	Treatment combinations	r.q.v. Mixture 1/1	r.q.v. Mixture 2/1	r.q.v. Mixture 3/1	r.q.v. Total/1
7	(1)	0.390	0.524	0.713	1.627
3	a	0.622	0.610	0.681	1.912
8	b	0.500	0.648	0.649	1.797
4	ab	0.634	0.790	0.660	2.084
1	c	0.659	0.800	0.681	2.139
6	ac	0.780	0.743	0.840	2.364
5	bc	1.000	1.000	1.000	3.000
2	abc	0.768	0.714	0.798	2.280

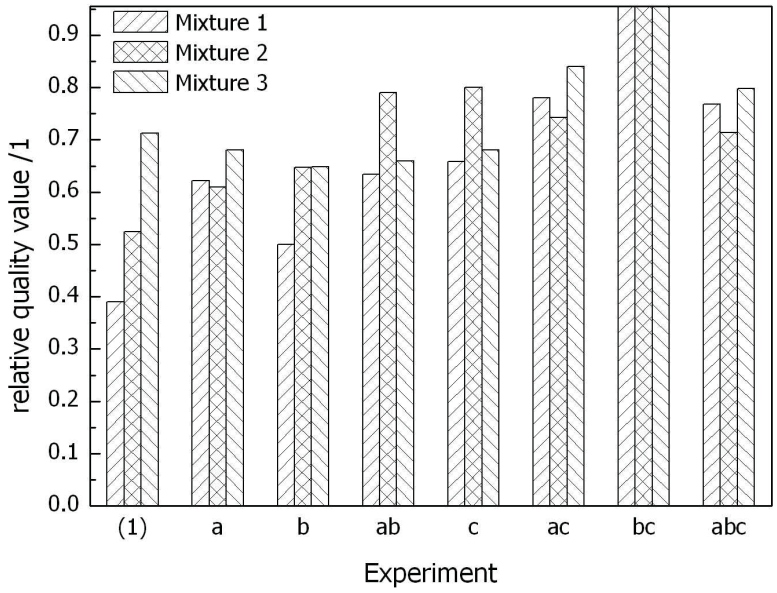

Fig. 4.2: Quality bars obtained from all treatment combinations for each sample.

effects and interactions can be computed according to literature.[43] The explicit values for the effects and interaction are given in Table 4.4.

Tab. 4.4: Solved Effects and Interactions referring to Coded Variables Obtained by Using the Calculation Concept given in Reference[43] (see text)

Effect, Interaction	Effect, Interaction / 1 (coded variables)
A	0.008
B	0.093
C	0.197
AB	-0.078
AC	-0.089
BC	0.036
ABC	-0.079

The computation of the analysis of variance and application of the three factor analysis of variance model to the effects obtained, indicates that a variation of the selected input parameters will significantly influence the quality of the CRYSTAF curve. The results of the analysis of variance are illustrated in Table 4.5. For each effect the sum of squares, degrees of freedom, mean square and test statistics are given. As confidence interval for main effects, $\alpha = 1\%$ and as confidence interval for interaction $\alpha = 10\%$ were chosen.[43]

The test of the constraint $F_0 \geq F_{1-\alpha}$ of each effect and interaction leads to the significant effects and interaction on CRYSTAF quality. As Table 4.5 shows, the only significant main effect is the stirring speed (C). This leads to the argumentation that for the chosen variable intervals, stirring speed is the most important parameter referring to the quality of fractionation in polymer solutions.

The only significant interactions are cooling rate AB, AC, and ABC. Thus the interaction of the cooling rate with start stabilization temperature (AB), cooling rate with stirring speed (AC), cooling rate with start stabilization temperature and stirring speed (ABC) are influencing the quality of CRYSTAF curve remarkably. The obtained information allows the composition of the model response function $\hat{y}$ given in Equation (4.4). The variables of the model function x_1, x_2, x_3 are defined in the coded interval $[-1, +1]$.

$$\hat{y} = 0.717 + 0.03924x_3 - 0.039x_1x_2 - 0.045x_1x_3 - 0.039x_1x_2x_3 \tag{4.4}$$

4.2.2 Optimization of the model function

By applying the optimization discussed in paragraph "Modeling" to the response function $\hat{y}$ the maximum of the response function in the closed set Ω can be calculated. An example snapshot of the sliced Ω can be seen in Figure 4.3. This graphic is only one

Tab. 4.5: Analysis of Variance of the Calculated Mean Effects and Interaction according to Reference[43]

effects, interactions	Sum of squares	Degrees of freedom	Mean square	F_0	$F_{1-\alpha}$ $1-\alpha = 1\%$ main effects $1-\alpha = 10\%$ interactions
A	0.000253	1	0.000253	0.04	11.26
B	0.052164	1	0.052164	8.01	11.26
C	0.232797	1	0.232797	35.76	11.26
AB	0.036958	1	0.036958	5.68	3.46
AC	0.047554	1	0.047554	7.30	3.46
BC	0.007909	1	0.007909	1.21	3.46
ABC	0.037293	1	0.037293	5.73	3.46
Error	0.104162	16	0.006510		
Total	0.519090	24			

snapshot of the whole experimental mathematical series. This and all other visualizations of the quality color field show that the maximum of $\hat{y}$ can be found in the upper left corner of Figure 4.3. As a result the coded variables $x_1 = -1$, $x_2 = 1$ and $x_3 = 1$ define the highest value of quality. By a linear transformation of the coded variables the factor quantities, which lead to the CRYSTAF curve with the highest quality can be found.

Thus a cooling rate of 0.1 °C/min, a start stabilization temperature of 140 °C and a stirring speed of 150 rpm are the optimal operating conditions of CRYSTAF if the set Ω is observed.

4.2.3 Experimental interpretation of the simulation results

The abstract model delivers the optimal operating conditions which are now applied to the CRYSTAF apparatus aiming in the verification of the mathematical model results. For this purpose the pure components of the mixtures, matrix polymer as well as modifier (see Table 3.4) are measured by CRYSTAF with the calculated optimal conditions, leading to the profiles $\gamma_1(T)$ for the matrix polymer and $\gamma_2(T)$ for the respective modifier, where T is the temperature in $°C$. With respect to the weight factors w_1 (matrix polymer: 0.8) and w_2 (modifier: 0.2) for the mixing ratio of the two components (see Table 3.4) the resulting CRYSTAF profile $\Gamma(T)$ of the blend can be calculated according to Equation (4.5):

$$\Gamma(T) = \gamma_1(T)\, w_1 + \gamma_2(T)\, w_2 \tag{4.5}$$

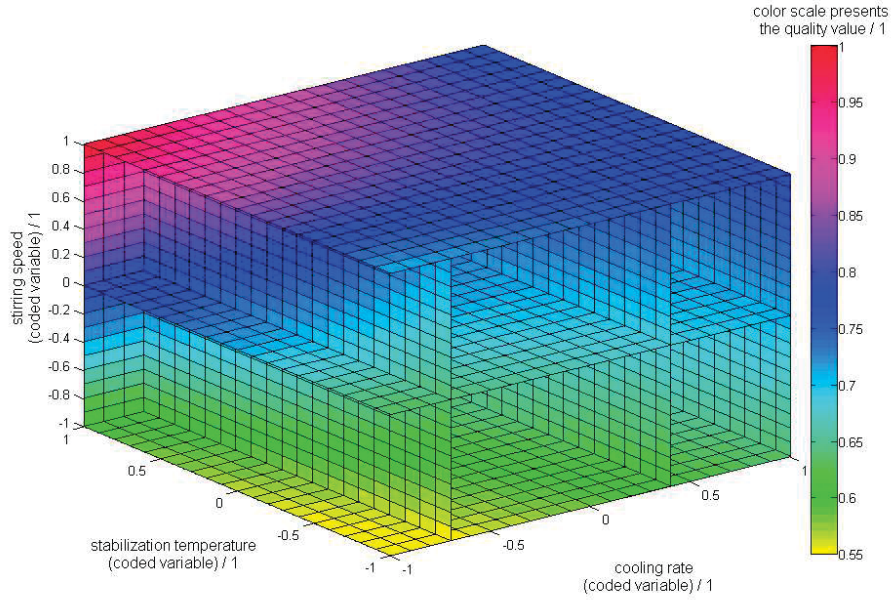

Fig. 4.3: Snapshot of the experimental mathematical slicing of the CRYSTAF color field in coded variables (MATLAB R2007b).

$\Gamma(T)$ is the ideal CRYSTAF profile of the compounded mixture which should be experimentally obtained when the calculated optimal operating conditions are applied to CRYSTAF. Depending on the selected operating conditions, the quality of fractionation of all three samples show the same tendency (see Figure 4.2). Exemplified by Mixture 2 the measured profiles $\gamma_1(T)w_1$ and $\gamma_2(T)w_2$ as well as the calculated $\Gamma(T)$ are depicted in Figure 4.4. $\Gamma(T)$ shows three distinctive peaks at temperatures of 66 and 77 $°C$ mainly resulting from the RACO and 83 $°C$ mainly resulting from the modifier component PE-LLD.

Figure 4.5 shows the CRYSTAF profile of Mixture 2 which was measured using a standard method defined in collaboration with PolymerChar. By a comparison with the calculated profile in Figure 4.4 it can be easily seen that the resolution of this profile is of low quality. The CRYSTAF curve shows one peak for the RACO at 64 $°C$ and one peak for PE-LLD at 79 $°C$.

In Figure 4.6 the CRYSTAF profile of Mixture 2 obtained using the optimized method is presented. A comparison with the calculated profile $\Gamma(T)$ (see Figure 4.4) shows that both profiles are nearly identical with peak maxima at 66, 77, and 83 $°C$. This is more clearly illustrated in Figure 4.7 by an overlay of $\Gamma(T)$ and the profiles measured at standard and optimized methods.

These experiments show that the optimized operating conditions calculated by the abstract model lead to a CRYSTAF profile, which is nearly identical to the ideal CRYSTAF profile $\Gamma(T)$.

In order to demonstrate the influence of stirring speed on the shape of the CRYSTAF

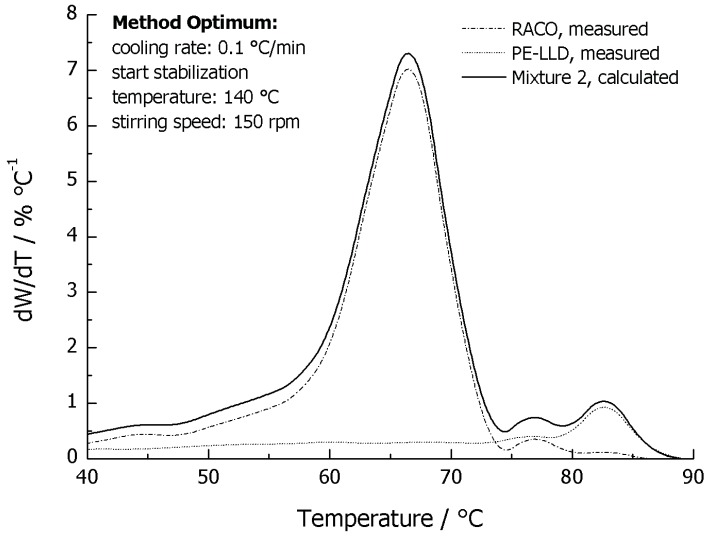

Fig. 4.4: Calculated Mixture 2 as a superposition of the weighted pure components (PE-LLD and RACO).

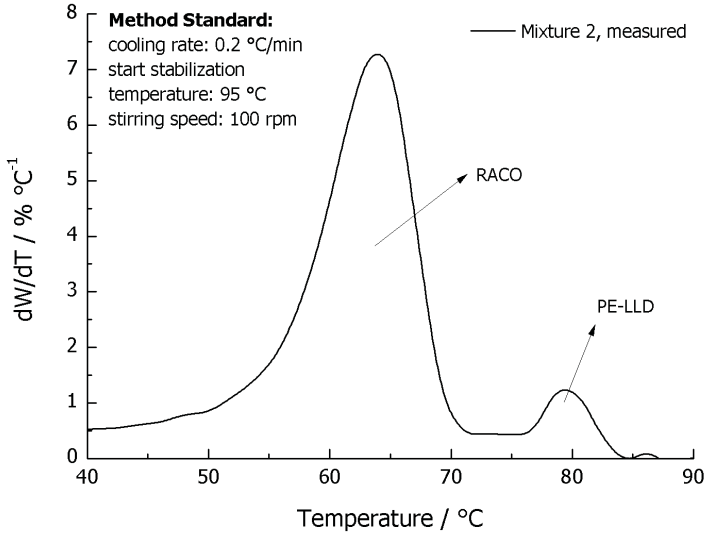

Fig. 4.5: CRYSTAF profile obtained using the standard method.

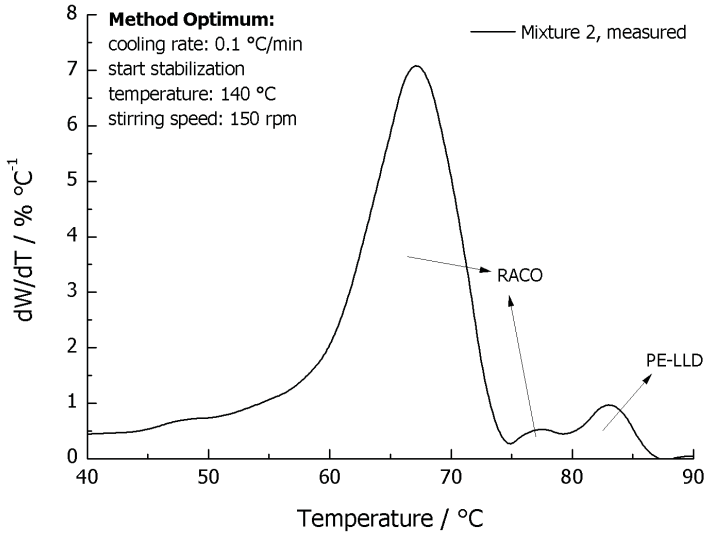

Fig. 4.6: CRYSTAF profile obtained using the optimized method.

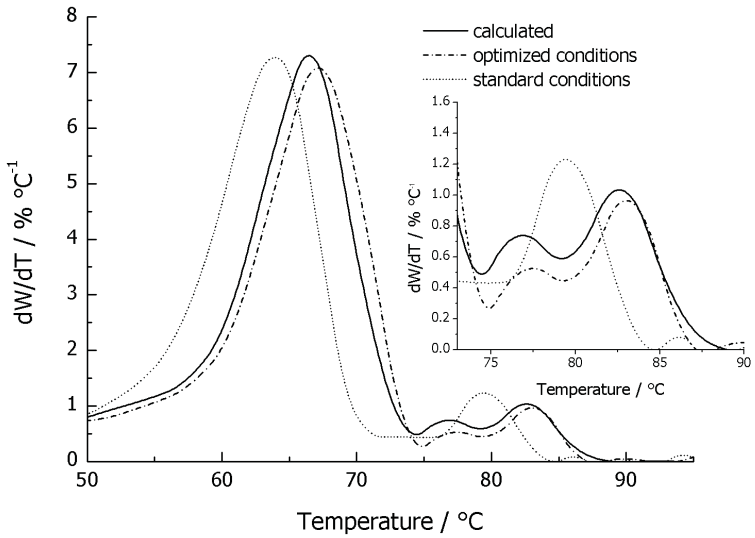

Fig. 4.7: Comparison of the calculated CRYSTAF profile and the profiles measured at standard and optimized conditions of Mixture 2.

curve, Mixture 1, 2, and 3 are measured at two stirring speeds, 50 and 150 rpm respectively, where the parameters of cooling rate and stabilization start temperature are kept constant. Figures 4.8, 4.9 and 4.10 illustrate this effect. Especially for Mixtures 2 and 3 a less resolved CRYSTAF profile and therefore less information about the composition of the referring blend is obtained at a stirring speed of 50 rpm. This can be easily seen by the disappearance of the peak at 77 °C in Figures 4.9 and 4.10.

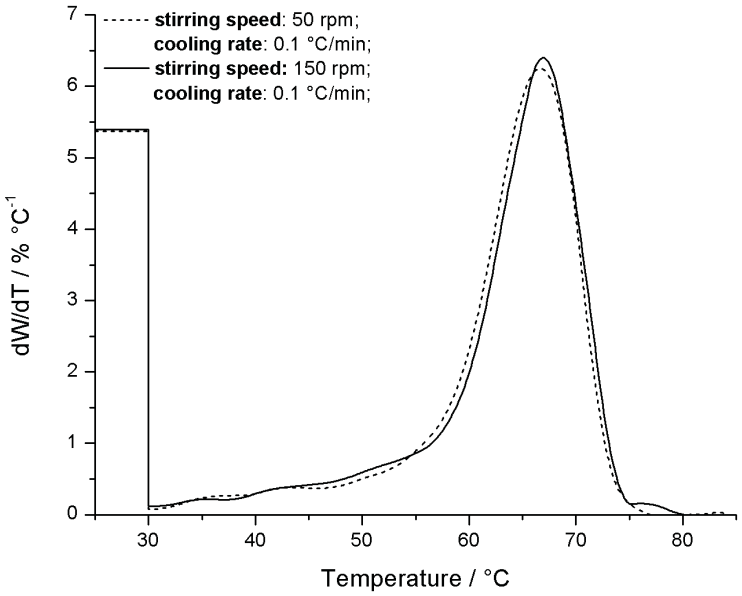

Fig. 4.8: CRYSTAF curves of Mixture 1 at varied stirring speed and constant cooling rate and start stabilization temperature.

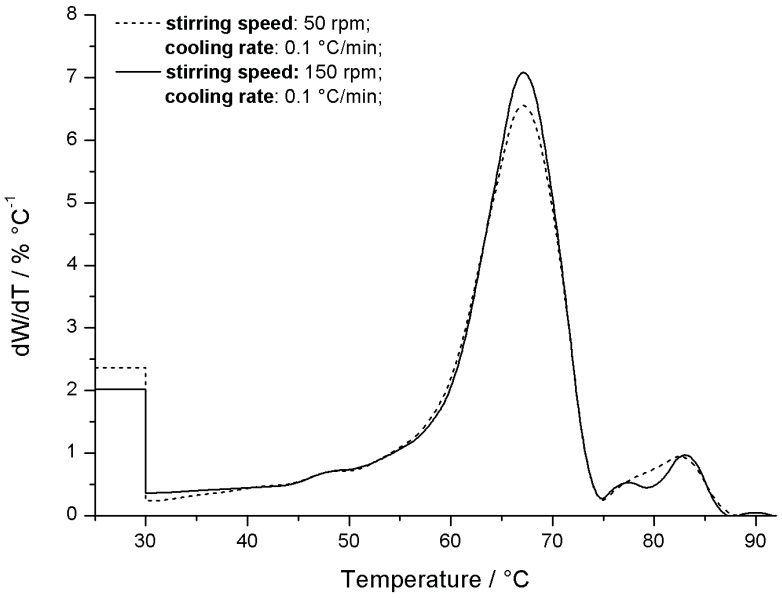

Fig. 4.9: CRYSTAF curves of Mixture 2 at varied stirring speed and constant cooling rate and start stabilization temperature.

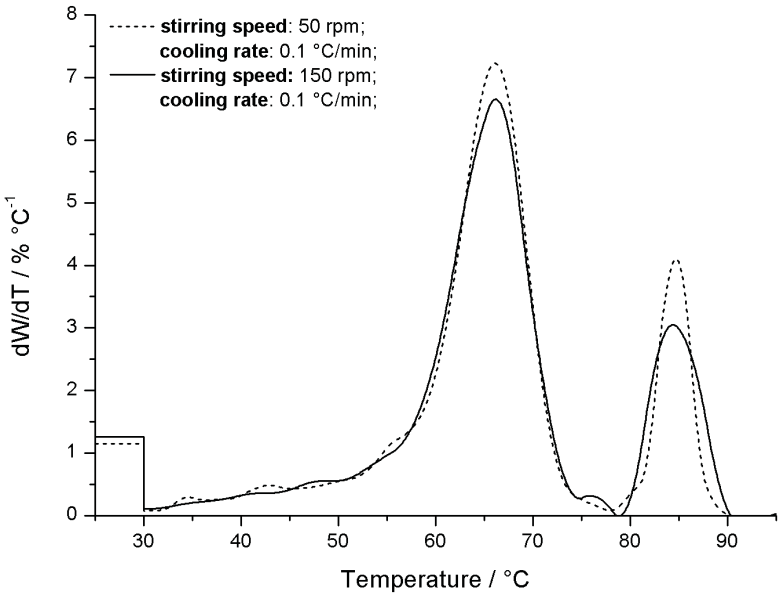

Fig. 4.10: CRYSTAF curves of Mixture 3 at varied stirring speed and constant cooling rate and start stabilization temperature.

4.3 Conclusion

The results of the mathematical model reveal that the precipitation of polymer blends from their solution is strongly influenced by the acceleration field in radial direction during the precipitation process. By application of the model, a new powerful method was implemented to CRYSTAF technique which assures a high quality separation of semicrystalline polymers and polymer blends. This could be experimentally verified on the basis of three different polyolefin blends.

Chapter 5

Comparison of TREF and CRYSTAF for characterizing polymer blends

A very interesting result referring to the characterization of polymer blends with TREF and CRYSTAF was recently brought up by Monrabal.[22] His investigation of a blend from a metallocene type homopolymer polypropylene with a small amount of a linear polyethylene shows that CRYSTAF separates the two components succesfully contrary to TREF which fails in the component separation process.[22] In this chapter TREF and CRYSTAF fractionation results according to Mixture 2 and Mixture 3 were compared. All investigations with TREF and CRYSTAF were done with optimized measurement conditions. The TREF operating conditions were set according to reference.[32] For CRYSTAF the new developed optimized parameter-set was used.

5.1 Experimental analysis conditions

The experimental conditions of TREF can be seen in Table 3.1 in Chapter 3. The optimized CRYSTAF operating conditions are illustrated in Table 3.3.

Tab. 5.1: Optimized Conditions of aCRYSTAF Temperature Profile (Maximum Temperature: 171 °C, Top Oven Temperature 150 °C, Low Stirring: Continuous Mode (c), High stirring: Discontinuous Mode (d)

	dissolution	stabilization	analysis	cleaning
rate/ (°C/min)	20.0	-	0.10	-
temp./ (°C)	160.0	140.0	140.0-30.0	160.0
stirring/ (rpm)	200.0 (d)	200.0 (d)	150.0 (c)	200.0 (d)

5.2 Results of the TREF-CRYSTAF-Comparison

5.2.1 TREF-Profiles of Mixture 2 and Mixture 3

Figure 5.1 and 5.2 present the TREF curves of Mixture 2 and Mixture 3. In Figure 5.1 the TREF curve characterizes a peak maximum at 32.5 °C which shows the rubbery phase of the sample with an amount of 13 wt.-%. In Figure 5.1 a second peak maximum for the RACO and PE-LLD phase with an amount of 87 wt.-% can be seen at a temperature of 102.6 °C.

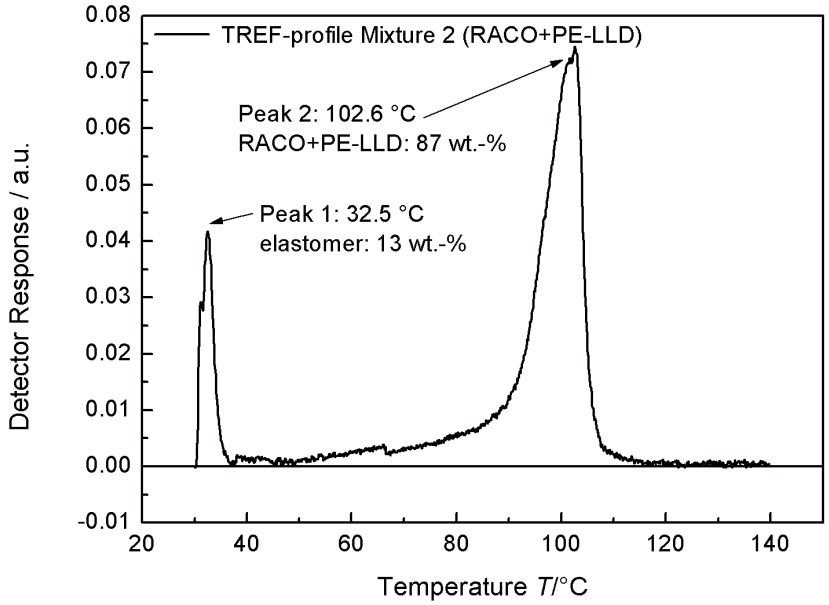

Fig. 5.1: TREF-profile of Mixture 2 measured with optimized operating conditions according to reference,[32] measured by C.Kock and T.Ehgartner.

The TREF characterization of Mixture 3 (see Figure 5.2) shows two different peaks as well. The first peak maximum at a temperature of 30.8 °C includes 7 wt.-% (rubbery phase) of the whole sample, the second peak includes 93 wt.-% of the sample (RACO+PE-HD phase) and has a peak maximum at 99.7 °C.

Both diagrams show clearly, that RACO mixed with PE-LLD and RACO mixed with PE-HD are not separable by TREF. In Figure 5.1 there is no separation observable, in Figure 5.2 a marginal marked shoulder coming from PE-HD can be seen as an initial sign of a phase separation process.

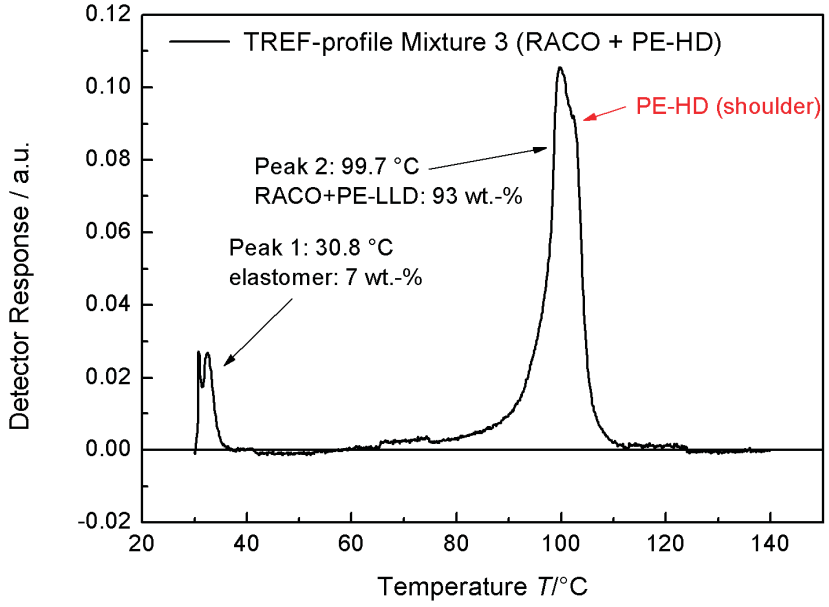

Fig. 5.2: TREF-profile of Mixture 3 measured with optimized operating conditions according to reference,[32] measured by C.Kock and T.Ehgartner.

5.2.2 CRYSTAF-Profiles of Mixture 2 and Mixture 3

Figure 5.3 and 5.4 illustrate the analytical CRYSTAF curves of Mixture 2 and Mixture 3 with optimized operating conditions. In Figure 5.3 the rubbery phase amounts to 11 wt.-%. Two further peaks can be seen, the first peak maximum at 67.1 °C refers to the RACO and the low density part of the PE-LLD with an amount of 82 wt.-%. The second peak maximum at 83.2 °C with an amount of 7 wt.-% shows the higher density part of the PE-LLD.

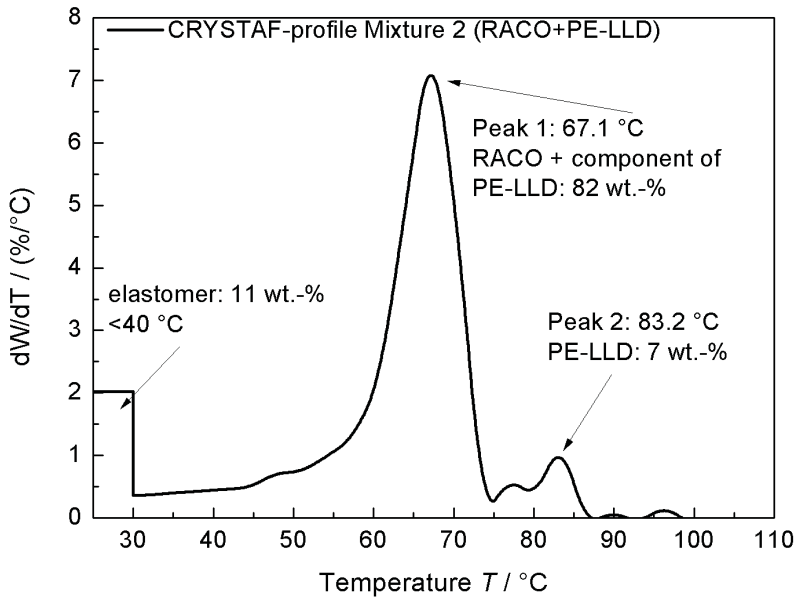

Fig. 5.3: CRYSTAF-profile of Mixture 2 measured with optimized operating conditions.

In Figure 5.4 the rubbery phase amounts to 8.3 wt.-%. Two further peaks can be seen, the first peak maximum at 66.1 °C refers to the RACO with an amount of 73.2 wt.-%. The second peak maximum at 84.3 °C with an amount of 18.5 wt.-% shows the PE-HD.

For both samples, Mixture 2 and Mixture 3 the CRYSTAF curves show an ideal separation process of the base polymer and the modifier.

In Figure 5.5 the base polymer (RACO) measured by TREF and CRYSTAF is compared. TREF as well as CRYSTAF show a very similar mesurement curve according to the curve structure. However, a remarkable peakshift of 35.1 °C between the two curves can be observed.

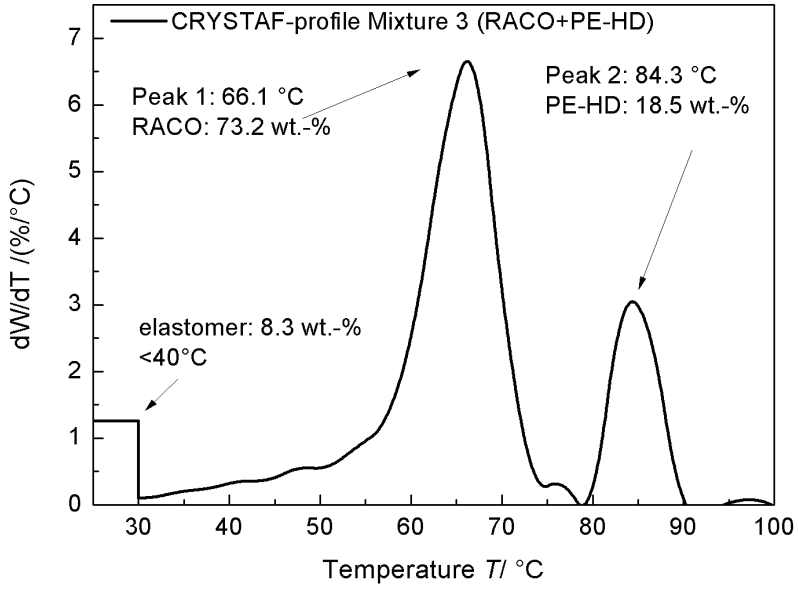

Fig. 5.4: CRYSTAF-profile of Mixture 3 measured with optimized operating conditions.

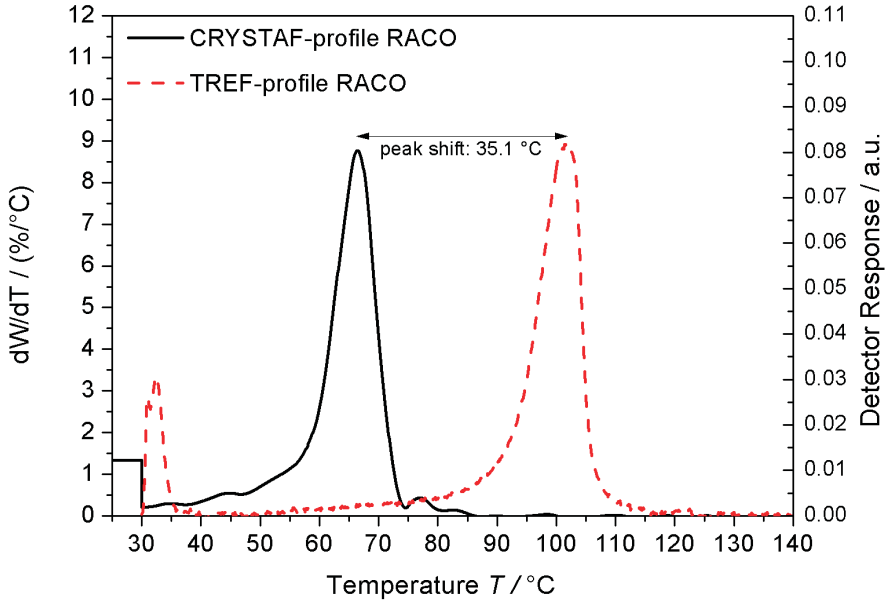

Fig. 5.5: Comparison of the TREF- and CRYSTAF-profile of the base polymer (RACO) shows a peak shift referring to the different measurements techniques.

5.3 Conclusion

By measuring the pure components (base polymer and modifier) examplified for the base polymer in Figure 5.5 of Mixture 2 and Mixture 3, TREF and CRYSTAF lead except for the typical temperature shift to similar measured curves. By characterizing the polymer blends with TREF and CRYSTAF the resulting curves show remarkable differences between the two separation techniques. With an optimized TREF analysis of polymer blends basing on a RACO as matrix polymer and small amounts of polyethylene as modifier (see Figure 5.1 and 5.2) it is impossible to fractionate the phases of the blended components. Contrary to TREF analysis, optimized CRYSTAF analysis of the same samples lead to an ideal phase separation of base polymer and modifier (see Figure 5.3 and 5.4) and allows a further off-line analysis of the fractionated components. Therefore, also for RACO as base polymer and polyethylene as modifier TREF and CRYSTAF lead to very different measurement profiles.

Chapter 6

Conclusion and Discussion

Goal of this Master Thesis was to find the experimental parameters which influence the CRYSTAF separation process and the development of an optimized separation method. This was done by the use of a coupling between a statistic mathematical model with an experimental investigation, which is a modern way for finding general significant experimental influence parameters. This approach delivered that the stirring speed in CRYSTAF analysis is for small cooling rate intervals the main influence factor on the separation process. Using this factor for optimization a characterizing method for CRYSTAF with an ideal phase separation for RACO-PE blends was developed. The studies also show that TREF is not successful in the fractionation of RACO-PE blends. The failure of phase separation by TREF was recently shown for polypropylene homopolymers blended with small amounts of linear polyethylene through B.Monrabal[22] as well. Also for polypropylene homopolymers blended with small amounts of linear polyethylene the CRYSTAF fractionation leads to a good phase separation. Indeed CRYSTAF and TREF bases on the same fractionation mechanism but the current study shows that the big difference in the results between the two characterization techniques are in the experimentel conditions. In TREF the polymer sample is not affected by an radial acceleration field during the precipitation and elution process, which is contrary to CRYSTAF. This fact and the results in this thesis lead to the argumentation that the reason for better phase separation and therefore, measurement profiles of CRYSTAF by analysing polymer blends lies in the acceleration force affecting the molecules during the measurement process. The physical interpretation of the effect of acceleration force on molecules during the phase separation could not be clarified in this study. However, this results open a field of further investigations referring to differences in the phase separation and co-crystallization of polymer blends according to the molecular radial acceleration force during the separation.

Chapter 7

Bibliography
List of Figures
List of Tables

Bibliography

[1] P.S.Chum and K.W.Swogger, "Olefin polymer technologies - History and resent progress at The Dow Chemical Company," *J.Prog.Polym.Sci.*, vol. 33, pp. 797–819, 2008.

[2] L.Wild, T.R.Ryle, D.C.Knobeloch, and I.R.Peat, "Determination of Branching Distribution in Polyethylene and Ethylene Copolymers," *J.Polym.Sci. Polym. Phys. Ed.*, vol. 20, pp. 441–455, 1982.

[3] K.F.Freed, "Phase Behaviour of Polymer Blends," *Adv.Polym.Sci.*, vol. 183, pp. 1–61, 2005.

[4] D.A.Thomas and L.H.Sperling, "Polymer Blends, Interpenetrating Polymer Networks," *Academic Press, New York SanFrancisco London*, vol. 2, pp. 2–31, 1978.

[5] L.A.Utracki, *Polymer Alloys and Blends, Thermodynamics and Rheology.* Hanser Publishers, Munich Vienna New York, 1989.

[6] D.R.Paul, "Background and Perspective," *Academic Press, New York SanFrancisco London*, vol. 1, pp. 2–14, 1978.

[7] P.J.Flory, *Principles of Polymer Chemistry.* Cornell University Press Ithaca and London, 1953.

[8] P.D.Gennes, *Scaling Concepts in Polymer Physics.* Cornell University Press, Ithaca and New York, 1979.

[9] K.Binder, "Phase transitions in polymer blends and block copolymer melts: Some recent developments," *Adv.Polym.Sci.*, vol. 112, pp. 181–299, 1994.

[10] W.W.Yau, J.J.Kirkland, and D.D.Blys, *Modern Size-Exclusion Liquid Chromatography.* John Wiley and Sons: New York Chichester Brisbane Toronto, 1979.

[11] G.Glöckner, *Polymer Characterization by Liquid Chromatography.* Elsevier: Amsterdam, 1987.

[12] J.Janca, *Field-Flow Fractionation, Analysis of Macromolecules and Particles.* Chromatographic Science Series, Volume 39, NewYork, 1988.

[13] W.Holtrup, "Zur Fraktionierung von Polymeren durch Direktextraktion," *Macromol.Chem.*, vol. 178, pp. 2335–2349, 1977.

[14] L.Wild, "Temperature Rising Elution Fractionation," *Adv.Polym.Sci*, vol. 98, pp. 1–47, 1991.

[15] J.B.Soares and A.E.Hamielec, "Temperature rising elution fractionation of linear polyolefins," *Polymer*, vol. 36, pp. 1639–1654, 1995.

[16] B.Monrabal, "Crystallization Analysis Fractionation: A New Technique for the Analysis of Branching Distribution in Polyolefins," *J.Appl.Polym.Sci.*, vol. 25, pp. 491–499, 1994.

[17] H.Pasch, R.Brüll, U.Wahner, and B.Monrabal, "Analysis of polyolefin blends by crystallization analysis fractionation," *Macromol.Mater.Eng*, vol. 279, pp. 46–51, 2000.

[18] C.Gabriel and D.Lilge, "Comparison of different methods for investigation of the short-chain branching distrinution of lldpe," *Polymer*, vol. 42, pp. 297–303, 2001.

[19] L.J.D.Britto, J.B.P.Soares, A.Penlidis, and B.Monrabal, "Polyolefin Analysis by Single-Step Crystallization Fractionation," *J.Polym.Sci. Part B: Polym. Phys.*, vol. 37, pp. 539–552, 1999.

[20] J.B.Soares and S.Anantawaraskul, "Crystallization Analysis Fractionation," *J.Polym.Sci. Part B: Polym. Phys.*, vol. 43, pp. 1557–1570, 2005.

[21] J.Xu and L.Feng, "Application of temperature rising elution fractionation in polyolefins," *Eur.Polym.J.*, vol. 36, pp. 867–878, 2000.

[22] B.Monrabal, "Microstructure Characterization of Polyolefins.TREF and CRYSTAF," *Stud. Surface Sci. Cat.*, vol. 161, pp. 35–42, 2006.

[23] S.Anantawaraskul, J.B.P.Soares, and P.M.Wood-Adams, "Effect of Operation Parameters on Temperature Rising Elution Fractionation and Crystallization Analysis Fractionation," *J.Polym.Sci. Part B: Polym. Phys.*, vol. 41, pp. 1762–1778, 2003.

[24] S.Anantawaraskul, P.Somnukguandee, J.B.P.Soares, and J.Limtrakul, "Application of a Crystallization Kinetics Model to Simulate the Effect of Operation Conditions on Crystaf Profiles and Calibration Curves," *J.Polym.Sci. Part B: Polym. Phys.*, vol. 47, pp. 866–876, 2009.

[25] S.Anantawaraskul, J.B.P.Soares, and P.Jirachaithorn, "A Mathematical Model for the Kinetics of Crystallization in Crystaf," *Macromol. Symp.*, vol. 257, pp. 94–102, 2007.

[26] S.Anantawaraskul, J.B.P.Soares, , P.Jirachaithorn, and J.Limtrakul, "Mathematical modeling of crystallization analysis fractionation of ethylene/1-hexene copolymers," *J.Polym.Sci. Part B: Polym. Phys.*, vol. 45, pp. 1010–1017, 2007.

[27] S.Anantawaraskul, J.B.P.Soares, , P.Jirachaithorn, and J.Limtrakul, "Mathematical modeling of crystallization analysis fractionation (crystaf) of polyethylene," *J.Polym.Sci. Part B: Polym. Phys.*, vol. 44, pp. 2749–2759, 2006.

[28] G.Astarita, *Thermodynamics An Advanced Textbook for Cemical Engineers*. Plenum Press,New York and London, 1989.

[29] P. J. Flory, "Thermodynamics of Crystallization in High Polymers. IV.A Theory of Crystaline States and Fusion in Polymers, copolymers, and Their Mixtures with Diluents," *J.Chem.Phys.*, vol. 17, p. 223, 1949.

[30] U. W. Gedde, *Polymer Physics*. Kluwer Academic Publishers Dordrecht, 2001.

[31] G. Strobl, *Physik kondensierter Materie: Kristalle, Flüssigkeiten, Flüssigkristalle und Polymere*. Springer-Verlag Berlin-Heidelberg-NewYork, 2002.

[32] N.Aust, M.Gahleitner, K.Reichelt, and B.Raninger, "Optimization of run parameters of temperature-rising elution fractionation with the aid of a factorial design experiment," *Polym. Test.*, vol. 25, pp. 896–903, 2006.

[33] V.Virkkunen *et al.*, "Tacticity distribution of isotactic polypropylene prepared with heterogeneous Ziegler-Natta catalyst. 2. Application and analysis of SSA data for polypropylene," *Polymer*, vol. 45, pp. 4623–4631, 2004.

[34] V.Virkkunen *et al.*, "Tacticity distribution of isotactic polypropylene prepared with heterogeneous Ziegler-Natta catalyst. 1. Fractionation of polypropylene," *Polymer*, vol. 45, pp. 3091–3098, 2004.

[35] P. Char, *Crystaf User Manual*. Polymer Char,Valencia,Spain, 2006.

[36] S.Anantawaraskul *et al.*, "Effect of molecular weight and average comonomer content on the crystallization analysis fractionation CRYSTAF of ethylene alpha-olefin copolymers," *Polymer*, vol. 44, pp. 2393–2401, 2003.

[37] R.Bruell *et al.*, "Investigation of Melting and Crystallization Behavior of Random Propene/alpha-Olefin Copolymers by DSC and CRYSTAF," *Macromol.Chem.Phys.*, vol. 202, pp. 1281–1288, 2001.

[38] S.Filho *et al.*, "Measurement and mathematical modeling of molecular weight and chemical composition distribution of ethylene/alpha-olefin copolymers synthesized with a heterogeneous Ziegler-Natta catalyst," *Macromol.Chem.Phys.*, vol. 201, pp. 1226–1234, 2000.

[39] P. Char, *TREF User Manual*. Polymer Char,Valencia,Spain, 2006.

[40] D.Montezinos *et al.*, "The Use of Ruthenium in Hypochlorite as a Stain for Polymeric Materials," *J.Polym.Sci. Polm. Let. Ed.*, vol. 23, pp. 421–425, 1985.

[41] C.Kock, A.Schausberger, N.Aust, M.Gahleitner, and E.Ingolic, *Polypropylene-Polyethylene Melts: Phase Structure Determination by Rheology.* AIP Conference Proceedings 1027 (15th International Congress on Rheology), 2008, Publisher: American Institute of Physics, 2008.

[42] M.Steinhauser, *Computational Multiscale Modeling of Fluids and Solids Theory and Applications.* Springer XVIII Edition, 2008.

[43] D.C.Montgomery, *Design and Analysis of Experiments.* John Wiley and Sons, Third Edition, 1991.

[44] W.G.Box and J.S.Hunter, *Statistics for Experimenters, An Introduction to Design, Data Analysis, and Model Building.* John Wiley and Sons, New York, 1978.

[45] B.R.Kowalski, *Chemometrics, Mathematics and Statistics in Chemistry, Volume 138 of Nato ASI(Advanced Science Institutes) Series C: Mathematical and Physical Science.* D.Reidel Publishing Company,Dordrecht, 1984.

[46] J.E.Dennis and R. B. Schabel, *Numerical methods for unconstrained optimization and nonlinear equations.* SIAM, 1996.

List of Figures

List of Tables